FACULTY OF HEALTH AND MEDICAL SCIENCES
UNIVERSITY OF COPENHAGEN
DEPARTMENT OF LARGE ANIMAL SCIENCES

Master's thesis

Eva Zander Hesselkilde

In Vitro Characterization of the Equine Cardiac Ion Channels

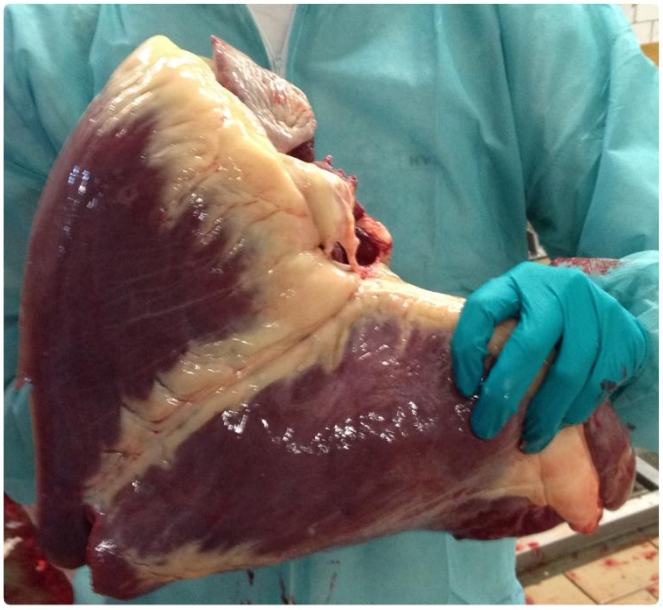

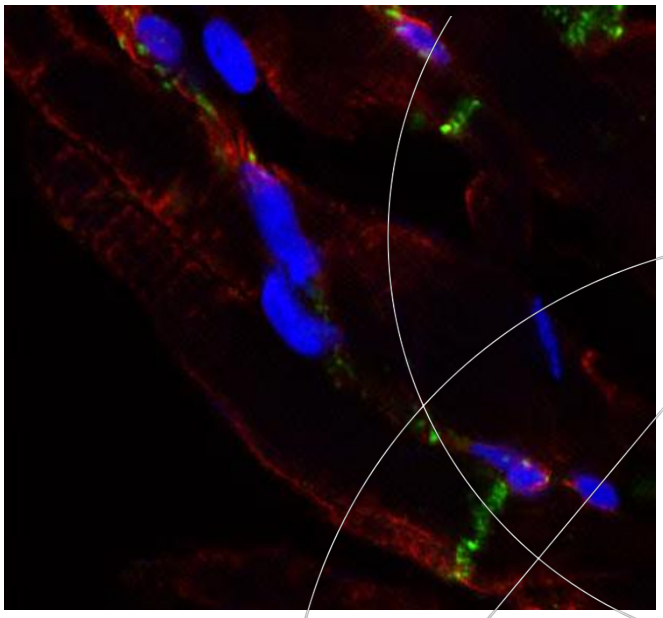

Academic advisors: Rikke Buhl, Professor (MSO), DVM, PhD
Thomas Jespersen, M.Sc.PhD, Dr.Med
Maria Mathilde Haugaard, DVM, PhD student

Submitted: 10/04/14

Preface

By this dissertation, I complete the Master's degree in Veterinary Medicine at the Faculty of Health and Medical Sciences, University of Copenhagen. It describes the experimental work carried out during November 2013 – February 2014, at the Department of Large Animal Sciences and Department of Biomedical Sciences. The thesis accounts for 30 ETCS points and is directed at anyone with an interest in equine cardiology.

For future publication the thesis is written in English and as a scientific paper. The introduction and method section is extended to provide a theoretical foundation on the equine cardiology and the methods used.

My work was accepted for chaired poster presentation on the European Cardiac Arrhythmia Society congress and was presented in Munich, March 2014.

I kindly thank my academic advisors; Rikke Buhl, Professor (MSO), DVM, PhD, Thomas Jespersen, M.Sc., PhD, Dr .Med and Maria Mathilde Haugaard, DVM, PhD student, for everlasting support and expert guidance. Also Thomas Hartig Braunstein, M.Sc., PhD and the rest of the staff in Core Facility for Integrated Microscopy at Department of Biomedical Sciences, University of Copenhagen, deserves my gratitude for their guidance and scientific advice on confocal imaging. Finally, thanks are given to all the PhD students and staff at the Membrane Protein Physiology group for creating an inspiring and instructive environment.

April 10TH 2014

_____

Eva Zander Hesselkilde

Zqh762

Abbreviations

AA: Amino acid

Ab: antibody

Ach: Acetylcholine

ACTB: Actin, beta

AF: Atrial fibrillation

AP: Action potential

APD: action potential duration

BLAST: Basic local alignment search tool

cDNA: Complementary DNA

C_t: Threshold cycle

dATP: Deoxyadenosine triphosphate

dCTP: Deoxycytidine triphosphate

dGTP: Deoxyguanosine triphosphate

dTTP: Deoxythymidine triphosphate

EtBr: Ethidium bromide

FAM: 6-carboxyflourescein

Ig: Immunoglobulin

LA: Left atrium

LSM: Laser scanning microscope

LV Endo: Left ventricular endocardium

LV Epi: Left ventricular epicardium

LV Mid: Left ventricular midmyocardium

MYH7: Myosin, heavy 7

PBS: Phosphate buffered saline

qPCR: Quantitative polymerase chain reaction

RA: Right atrium

RT: Reverse transcriptase

RV: Right ventricle

ΔC_t: Delta C_t

Abstract

Increased focus on prevalence and causes of cardiac arrhythmias in horses has aroused in recent years. Unlike other animals, atrial fibrillation (AF) is a frequent arrhythmia in horse. Also, horses with non-diseased hearts can be electrical triggered into shorter and longer periods of AF. Lately there has been increasing interest in the small-conductance Ca^{2+}-activated K^{+} (SK) channels as a specific target of the atria. At the Department of Large Animals Sciences, University of Copenhagen, successful clinical trials using drugs targeting the SK channels to abrogate induced AF has been performed. Such pharmacological observations suggest that equine hearts may constitute a *bona fida* model of human AF. To further investigate whether horses can be used to improve treatment of human arrhythmias knowledge about the equine cardiac ion channels are needed.

The aim of this study is to quantify the presence, expression level and cellular and regional distribution of the most prominent calcium, sodium and potassium ion channels in the horse heart. The genes of interest are: KCNN1 (SK1), KCNN2 (SK2), KCNN3 (SK3), KCND3 (Kv4.3), KCNJ2 (Kir2.1), KCNIP2 (KChiP2), KCNQ1 (Kv7.1), KCNA5 (Kv1.5), KCNJ3 (GIRK1), KCNJ5 (GIRK4), KCNH2 (ERG1), CACNA1C (Cav1.2), and SCN5A (Nav1.5).

Methods: Quantitative real time PCR (qPCR) was conducted on cardiac tissue collected from 6 different atrial (RA and LA) and ventricular (RV and endo, mid and epi LV) locations from 6 euthanized horses (3.4 ± 0.2 kg). Immunohistochemistry was performed on 12 μm cryosections from both right atrial and ventricular preparation. SK2 channels were stained with a previously tested SK2-antibody, to document distribution and localization of this protein in the equine heart.

Results: Quantifications of the major cardiac ion channels in the equine heart revealed an expression pattern which to a large extent resembles the human expression profile. These results thereby support the resemblance between human and equine hearts.

Resume

Veterinær forskning har den seneste tid haft større og større fokus på arytmier i heste. Modsat andre dyr er atrieflimmer (AF) en hyppig diagnosticeret lidelse. AF opstår spontant men kan også induceres i hest ved elektrisk stimulation af hjertet. Som led i at optimere AF behandlingen har der været stor fokus på "small-conductance Ca^{2+}-activated K^+ channels" – de såkaldte SK kanaler, da de menes at være atriespecifikke. På Universitetshospitalet for Store Husdyr, Københavns Universitet har *in vivo* forsøg vist, at lægemidler der modificerer SK kanalerne kan konvertere heste med induceret AF til sinus rytme. Disse farmakologiske observationer har ledt til den overbevisning, at hesten kan fungere som en dyremodel for mennesker. For at validerer dette, er der behov for en grundig karakterisering af ion kanalerne i hestens hjerte.

Formålet med dette studie var at undersøge ekspressions niveau samt den cellulære og regionale distribuering af de vigtigste calcium, natrium og kalium ion kanaler i hestens hjerte. De inkluderede gener er: KCNN1 (SK1), KCNN2 (SK2), KCNN3 (SK3), KCND3 (Kv4.3), KCNJ2 (Kir2.1), KCNIP2 (KChiP2), KCNQ1 (Kv7.1), KCNA5 (Kv1.5), KCNJ3 (GIRK1), KCNJ5 (GIRK4), KCNH2 (ERG1), CACNA1C (Cav1.2), and SCN5A (Nav1.5).

Metode: Vi brugte kvantitativ qPCR på hjertevæv fra seks heste, seks forskellig steder i hjertet (højre og venstre atrie, højre ventrikel samt endo-, mid og myokardie fra venstre ventrikel). Immunohistokemi blev udført på 12 μm cryosnit skåret af både højre atrie og højre ventrikel. Snittene blev farvet med SK2 antistoffer, der er valideret i tidligere forsøg. Immunohistokemi kan, modsat qPCR, beskrive lokaliseringen og distribueringen af selve proteinet.

Resultater: Kvantitativ analyse af the vigtigste ion kanaler i hestens hjerte viste et ekspressions mønster meget nær det humane. Dette underbygger teorien om at der er stor lighed mellem hestens og menneskets hjerte.

Table of Contents

Background

Increased focus on prevalence and causes of cardiac arrhythmias in horses has aroused in recent years (Barbesgaard, Buhl et al. 2010), (Leroux, Detilleux et al. 2013). Horses are known to develop both supraventricular and ventricular arrhythmias but several studies suggest that atrial fibrillation (AF) is the most clinically relevant arrhythmia (Leroux, Detilleux et al. 2013), (Holmes, Henigan et al. 1986), (Ohmura, Hiraga et al. 2003). Treatment of arrhythmia often involves antiarrhythmic drugs targeting cardiac ion channels but the knowledge about the molecular basis of the equine heart is limited. Lately, there has been increasing interest in the small-conductance Ca^{2+}-activated K^+ (SK) channels as a specific target of antiarrhythmic drugs (Nattel 2009). Cardiac SK channels have been demonstrated in several species (Xu, Tuteja et al. 2003), (Tuteja, Xu et al. 2005), (Diness, Sorensen et al. 2010). At the Department of Large Animals Sciences, University of Copenhagen, successful clinical trials using drugs targeting the SK channels have terminated induced AF, suggesting that SK channels are expressed in the equine heart. To verify the presence of SK channels and to aid treatment of equine arrhythmia in general a thorough characterization of the equine cardiac ion channels have been performed.

This report will focus on the ion channels investigated and the methods used. A brief review of the function the heart and the ion channels are given below. The review is mainly based on human literature due to the limited knowledge about the equine cardiac electrical properties.

Aim

The aim of this study was to characterize the expression level and cellular and regional distribution of the most prominent calcium, sodium and potassium ion channels in the equine heart. The genes (protein names) of interest are CACNA1C (Cav1.2), SCN5A (Nav1.5) KCND3 (Kv4.3), KCNIP2 (KChiP2), KCNA5 (Kv1.5), KCNH2 (ERG1), KCNQ1 (Kv7.1), KCNJ2 (Kir2.1), KCNJ3 (GIRK1) and KCNJ5 (GIRK4). In addition we wished to demonstrate the presence of the three isoforms of the small-conductance Ca^{2+}-activated K^+ channels; KCNN1 (SK1), KCNN2 (SK2) and KCNN3 (SK3).

Introduction

Cardiac action potential

Proper function of the heart is a result of a coordinated contraction of the cardiac muscle. The contraction of the cardiomyocytes is controlled by electrical signals recognized as cardiac electrical impulses in form of action potentials (AP). APs mediate release of cytosolic calcium triggering contraction. Myocardial activation is initiated by pacemaker cell in the sinoatrial node and is conducted through the atria to the atrioventricular node. Here the conduction is slowed before the impulses proceeds to the ventricles through the Bundle of Hiss and the Purkinje fibers. The slowed conduction in the atrioventricular node secures atrial-mediated filling of the ventricles prior to ventricular contraction that subsequently pumps blood into the vascular system. The electrical impulses can spread very rapidly because they are electrically coupled through connexins that allows various molecules and ions to pass freely between cells. The action potential is basically a reflection of the currents generated by the movement of ions across the cell membrane. Depolarization is the result of influx of Na^+ and Ca^{2+} whereas repolarization is mediated by K^+ efflux. The movements are primarily through ion channels that are membrane-embedded proteins activated upon stimuli and selectively allow passage of ions. In the heart the stimulus for activation and inactivation is primarily changes in voltage. The cardiac AP is very long compared to nerve cell AP and it allows the long lasting contraction crucial for normal function of the heart. Furthermore, the extended action potential keeps the myocardium refractory so that no new AP can be mediated and disturb the ongoing contraction. Several ionic currents are involved in the formation of the AP and they are described below.

Protein complexes mediating the cardiac action potential

The most prominent ion channels, the genes encoding them and the currents they produce are listed in Table. 1.

Gene	SCNA5	CACNA1C	KCND3	KCNIP2	KCNA5	KCNH2	KCNQ1	KCNJ2	KCNJ3	KCNJ5
Channel	Nav1.5	Cav1.2	Kv4.3	KChiP2	Kv1.5	Kv11.1	Kv7.1	Kir2.1	Kir3.1	Kir3.4
Current	I_{Na}	I_{CaL}	I_{to}	I_{to}	I_{Kur}	I_{Kr}	I_{Ks}	I_{K1}	I_{KACh}	I_{KACh}

Table. 1. *Cardiac ion channels, currents and genes contributing to action potential modulation*.

Due to the difference in protein expression throughout the heart the shape of the AP varies but the underlying mechanism is similar. The heterogeneity of AP waveforms in different anatomic regions of the heart is schematically illustrated in figure 1.

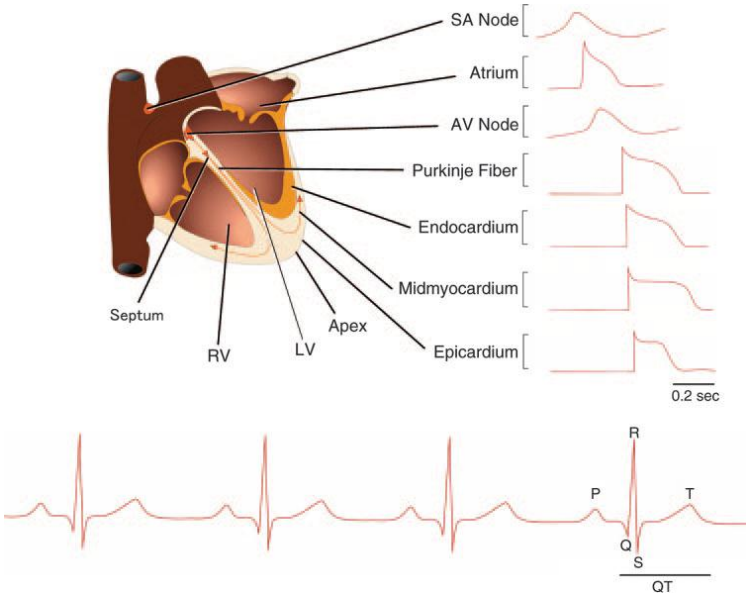

Fig. 1 *Electrical activity in the myocardium*. Top: Schematic illustration of a human heart. The shape of the AP varies in different regions due to difference in protein expression. Bottom: Surface electrocardiogram; Three sequential beats are displayed reflecting the relative muscle mass being either depolarized (P-wave and QRS complex) or repolarized (T-wave). Adapted from (Nerbonne and Kass 2005).

The morphology of the action potential is divided into five phases (0-4) each reflecting the underlying currents (Nerbonne and Kass 2005). Phase 0 describes the depolarization where the membrane potential changes from about - 85 mV to + 25 mV (Petitprez, Jespersen et al. 2008). Depolarization is initiated when the resting membrane reaches threshold (approximately -55 mV) causing a fast opening of sodium channels (Nav1.5) and allows a rapid inward movement of Na^+. The sodium channel deactivates after a few milliseconds mean while the transient outward potassium channels are activated. The currents from these potassium channels (I_{to}) are responsible for the partial repolarization characterizing phase 1 (Nerbonne and Kass 2005). The molecular entity underlying I_{to} is Kv4.3 encoded by KCND3 co-expressed with KChiP2, a Ca^{2+}-sensitive Kv channel-interacting protein encoded by KCNIP2 (An, Bowlby et al. 2000). I_{Kur} (Kv1.5) is reported to dominate the atria and is activated in the early phase of the AP. It is likely that this additional current contributes to the rapid repolarization seen in the atria compared to the ventricles (Fig. 1) (Nerbonne and Kass 2005). With a delay, membrane depolarization also activates L-type calcium channel Cav1.2 and Ca^{2+} enters the cell. L-type calcium channels are also called high voltage activated Cav channels as they activate at approximately – 20 mV (Bean 1985). Compared to the sodium channel, Cav1.2 is open for a relatively long period of time (~100 ms) (Bean 1985). The simultaneous influx of Ca^{2+} and efflux of K^+ leads to the long-lasting plateau seen in phase 2. When

I_{CaL} terminates, potassium efflux dominates and the final part of the repolarization (phase 3) occurs. It is mainly the rapid and slow delayed rectifier currents (I_{Kr} and I_{Ks}) and the inward rectifier (I_{K1}) currents that are responsible for phase 3 repolarization. I_{Kr} is conducted through the ERG1/ Kv11.1 channel and has a unique biphasic feature. ERG1 opens upon depolarization but is inactivated again shortly hereafter and remains in this state in the early phase 2 and thereby only contribute minor to the potassium efflux during the plateau phase. When membrane potential decreases the open Kv11.1 channels recover from inactivation and starts allowing efflux of K^+, thus contributes to repolarization (Trudeau, Warmke et al. 1995). The slow rectifier current, I_{Ks} is mediated via Kv7.1 and display a delayed activation compared to I_{Kr}. Opposite I_{Kr} there is no inward rectification evident for the I_{Ks} (Sanguinetti and Jurkiewicz 1992). Besides from terminating the action potential, I_{K1} is one of the primary currents setting the resting membrane potential (phase 4). The ion channel, Kir2.1, is an inward rectifier potassium channel; the channels are activated by repolarized potentials resulting in less current passing the membrane when it is depolarized than when it is repolarized. Kir3.1 and 3.4 are G-protein-regulated inwardly rectifying K^+ channels (also called GIRK) and their current (I_{KACh}) is also involved in controlling the resting membrane potential. Unlike most of the ion channels these are not voltage depended but activated by acetylcholine (Nerbonne and Kass 2005). A schematic overview of the ion channels and their effect on the action potential is presented in Fig. 2.

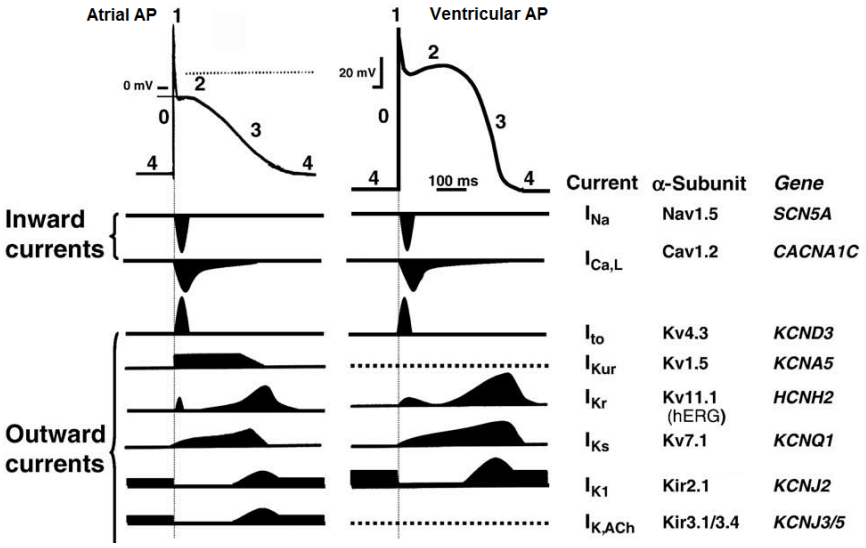

Fig.2 *Ion currents contributing to the modulation of action potential in atrial and ventricular cardiomyocytes*. The AP can be divided into five phases, 0-4. The inward sodium and calcium currents are responsible for the depolarization while several potassium currents are responsible for the repolarization. Figure modified from (Ravens 2010).

Small-conductance Ca^{2+}-activated K^+ (SK) channels are highly expressed in various tissues including smooth and skeletal muscle and neural tissue (Chen, Gorman et al. 2004). However, within the last few years, the interest of their functionally role in cardiac electrophysiology have increased. Their presence has been documented in several species (Diness, Sorensen et al. 2010), (Xu, Tuteja et al. 2003), (Tuteja, Xu et al. 2005). SK channels (SK_{Ca}) are voltage-independent but activated by intracellular Ca^{2+}. Due to the linking of fluctuations in intracellular calcium with membrane potassium conductance, SK channels are expected to participate in the repolarization of the action potential (Xu, Tuteja et al. 2003), (Tuteja, Xu et al. 2005). Studies have demonstrated that inhibiting SK2 channels have a greater effect on the atrial action potential than the ventricular action potential (Xu, Tuteja et al. 2003), (Diness, Sorensen et al. 2010), suggesting that SK channels, at least functionally, are atria-specific.

Disturbances in the ion currents described above will cause an unorganized electrical impulse propagation, uncoordinated muscle contraction and finally loss of cardiac pumping function. Irregular electrical activity of the heart is termed arrhythmia. Besides from reducing quality of life, arrhythmia proposes serious health hazards in both humans and horses. The following section will give a brief introduction to atrial fibrillation in horses since it is considered the most clinically relevant arrhythmia.

Arrhythmia in horses

Horses are particularly predisposed to AF because of their large atria and high vagal tone (Marr and Brown 2010). Dominance of the parasympathetic nervous system causes heterogeneity of the action potential duration (APD) and as a consequence a difference in the refractory periods in different areas of the heart. This results in an abnormal impulse propagation that favors AF (Dobrev, Carlsson et al. 2012). When the coordinated contraction responsible for ventricular filling is disrupted the heart needs to work harder to maintain adequate cardiac output. In situations where increased cardiac output is needed the heart cannot keep up and the clinical manifestation of AF is poor performance. Thus, AF is especially diagnosed in athletic horses but is otherwise frequently an incidental finding (Marr and Brown 2010). A recent published study showed a prevalence of AF of 0.02% in horses referred to the hospital concerning an abnormal cardiac auscultation. In comparison the prevalence of any ventricular arrhythmia was 0.0075% (Leroux, Detilleux et al. 2013). A study focusing on atrial fibrillation in Japanese racehorses suggested a prevalence of 0.29 % (Ohmura, Hiraga et al. 2003). Currently available treatment of AF is limited by moderate efficacy and severe

adverse effects. The adverse effects include life-threatening ventricular proarrhythmia because many of the antiarrhythmic drugs affect ions channels expressed in both atria and ventricles (Diness, Sorensen et al. 2010). Recently, the aim have therefore been to develop drugs targeting ion channels specifically expressed in the atria (Dobrev, Carlsson et al. 2012). Small-conductance Ca^{2+}-activated K^+ (SK) channels have been described in several species as, at least at the functional level, atrial specific and a promising therapeutic target (Nattel 2009). Unpublished data produced within the group, have shown that drugs modulating the SK channels can terminate induced atrial fibrillation in horses, suggesting that SK channels are present in the equine heart (unpublished data, M. Haugaard).

Despite the increased focus of cardiac arrhythmias in horses the scientific foundation is still weak. To establish the grounds for future research, a thorough characterization of the equine cardiac ion channels is needed. Comparing the equine ion channel distribution to the human distribution will not only improve the veterinary aspect in AF treatment, it will also determine if the horse can be used as an animal model for studies of human cardiac electrophysiology. We have characterized the expression level and distribution of several important ion channels in the equine heart using quantitative real time PCR (qPCR) and additionally proved the presence of SK channels using immunohistochemistry.

Materials and methods

Equine tissue samples

The heart tissue was collected from a slaughter house immediately after slaughter. 11 hearts were collected from horses of different breeds. All horses were visually inspected prior to slaughter. Six horses were auscultated and four had a brief (1-2 minutes) ECG recorded using the AliveCor Veterinary Heart Monitor (Model: AC-002). The AliveCor monitor is a cover for IPhones that records a single lead ECG when placed above the heart. Due to variation in the tissue quality (described in details in 'results') tissue from only six horses were used in the experiments. The six horses had a mean age of 9.2 years (range 4-14) consisting of one stallion and five mares. Permission was not required form the Danish Animal Experiments Inspectorate.

Immediately after meat inspection the hearts were collected and weighed. Larger chunks from the right and left atrial appendage and ventricles were dissected and placed in cold cardioplegic

solution. 4 mm biopsy punches were used to dissect tissue for qPCR which were placed in eppendorf tubes containing RNA*later®*-ICE (Ambion, USA). 8 mm biopsy punches were used to dissect the tissue later used for immunohistochemistry. Samples were obtained from the right atrial appendage (RA), left atrial appendage (LA), right ventricle (RV), left ventricular endocardium (LV Endo), left ventricular midmyocardium (LV Mid) and left ventricular epicardium (LV Epi). After dissection the tissue were stored on dry ice and later on – 80 degrees until usage.

Polymerase Chain Reaction

PCR is a cell-free way of cloning DNA sequences. It produces a large numbers of copies and effectively purifies the DNA so it can be comprehensively studied. It is a rapid and specific technique that allows amplification of a sequence from even small amounts of DNA. It is a process of several cycles and it leads to an exponential amplification of the target DNA (Strachan and Read 2011). Each cycle consist of three reactions; *denaturation*, *annealing* and *elongation*. Denaturation occurs when the temperature is raised high enough for the hydrogen bonds to break (~ 95°C) and there by separating the double stranded DNA. The temperature is then decreased which allows the primers to bind to the single stranded DNA. The primers are synthesized oligonucleotides that are complementary to the sequences flanking the target DNA. After annealing of the primers the elongation begins. The reaction mixture contains purified DNA polymerase and the four deoxynucleoside triphosphates dGTP, dATP, dCTP and dTTP which all together synthesize new DNA strands using the original DNA as templates. When the primers are designed, both the forward and reverse primer is orientated toward each other so that the newly synthesized DNA can serve as a template in the next cycle. The result is an exponential increase of the PCR product. After 20-40 cycles the DNA is usually transferred to agarose gels where it can be size-fractionated and visualized by the binding of ethidium bromide (EtBr) which fluoresces under ultraviolet light (Strachan and Read 2011). This method has a limited sensitivity and should only be used for qualitative analyses. In addition it is a time-consuming process and proposes a potential health hazard since EtBr is a potent mutagen (Singer, Lawlor et al. 1999). To avoid EtBr exposure and to quantify the DNA, real-time or quantitative PCR (qPCR) can be used. The qPCR machine detects the PCR product parallel to when the reactions occur. There are different methods to detect the quantity of the PCR product. In this project we used TaqMan® Gene Expression where TaqMan oligonucleotide probes are added to the reaction mixture. A 6-carboxyflourescein (FAM) fluorophore is attached to the 5´ end of the TaqMan probe and a quencher groups is attached to the

3´ end. When the probe is intact the quencher will absorb all the light from the fluorophore. During the annealing step of the PCR reaction the oligonucleotide will hybridize to a complimentary sequence of the single stranded DNA. When elongation proceeds the polymerase will cleave the TaqMan probe from the DNA and thereby separating the fluorophore from the quencher (Figure 3). The light from the fluorophore will no longer be absorbed by the quencher which allows the qPCR machine to detect the light and thereby quantify the amount of PCR product being synthesized (Strachan and Read 2011).

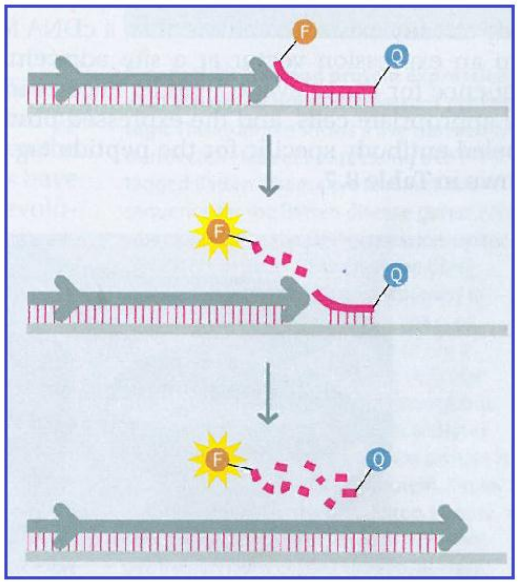

Fig. 3 *Hybridization of a TaqMan probe to a PCR amplicon*. When elongation proceeds the Fluorophore (F) and the quencher (Q) is separated from each other. Modified from (Strachan and Read 2011)

When qPCR is used to investigate gene expression it is preferable to extract mRNA from the tissue rather than DNA since the genome consists of thousands of genes that never will be transcribed let alone translated. It should however be noted that finding mRNA is not a conclusive prove of gene expression due to the multiple modifications of mRNA before protein expression that can lead to degradation or up regulation of either one. These modifications involve; microRNA-mediated splicing, post-transcriptional and post-translational modifications (Strachan and Read 2011).

To purify the RNA, tissue samples were homogenized with Tri Reagent® (Sigma-Aldrich, USA); a mixture containing guanidine thiocyanate and phenol, dissolving DNA, RNA and protein from the tissue. Chloroform was added to the sample to separate the products in three phases: the aqueous phase containing RNA, the interphase containing DNA and the organic phase which holds the proteins (Chomczynski and Sacchi 2006). The RNA was extracted and washed several times with

70% alcohols to avoid chemical reaction with phenol in the following steps. The quality of the RNA was evaluated on 1% agarose gels by adding 5µL sample and 2 µL RNA loading dye to each well verifying the presents of the ribosomal RNA 28S and 18S (Bustin and Nolan 2004). Concentration was estimated using the RNA ladder as a reference (150 ng/µL) (Fig. 7).

Before proceeding with the qPCR reaction the RNA must be copied into a complimentary DNA sequence (cDNA) using reverse transcriptase (RT) and random-sequence oligonucleotide primers. Following the manufacturer's instructions, cDNA was synthesized from 2 µg RNA using the High-Capacity cDNA Reverse Transcription Kit (Applied Biosystem, USA).

To replicate only the target sequence specific primers are required. All TaqMan assays (TaqMan® MGB probe and primers) were delivered from *Life Technologies*™. Primer sequences specific for SCN5A, KCNH2, KCNJ3, KCNQ1, KCNA5 and ACTB was designed by *Life Technologies*™. However, the equine sequences for KNCJ2, KCNJ5, KCNN1, KCNN2, KCNN3, KCND3, KCNIP3 and CACNA1C are listed as "predicted" in the National Center for Biotechnology Information's (NCBI) database why *Life Technologies*™'s software was not able to design specific primers for these genes. This was then done manually by the author using Primer Express® Software 3.0 (Applied Biosystems). The efficiency of each assay were evaluated by a serial dilution (1:1, 1:5, 1:25, 1:125, 1:625) using duplicate analyzes.

To correct for difference in the amount of input mRNA an endogenous reference gene was analyzed by RT-qPCR as well. We tested both myosin, heavy chain 7 (MYH7) and actin, beta (ACTB). ACTB was chosen as the only gene for normalization due to the poor uniform expression pattern of MYH7. Each of the 14 genes in the six different areas from six hearts was analyzed in triplets on the 7300 RT-qPCR System (Applied Biosystem, USA). In every experiment a negative control was included; three wells where no sample was added tested the plate for DNA contamination. The output of the qPCR analysis is threshold cycle (C_t) and is a log-linear plot of PCR signal (from the fluorophore) versus cycle number. The threshold is an arbitrary value set by the computer why this method only should be used as a comparative relative quantification method. Delta C_t (ΔC_t) is calculated by subtracting mean C_t of the target gene and the reference gene. The exponential data is then converted to linear form by the $100 * 2^{\Delta Ct}$ equation (Livak and Schmittgen 2001). An example for KCNJ5 in right atrium in horse_1 is given here: $C_{t(KCNJ5)} = 22.6$ and $C_{t(ACTB)} = 21.9 \Rightarrow \Delta C_t = 0.7$. The exponential data is then converted to linear form: $100 * 2^{0.7} = \underline{60.7.}$ Thus, low C_t is an expression for high cDNA level since threshold is reached fast.

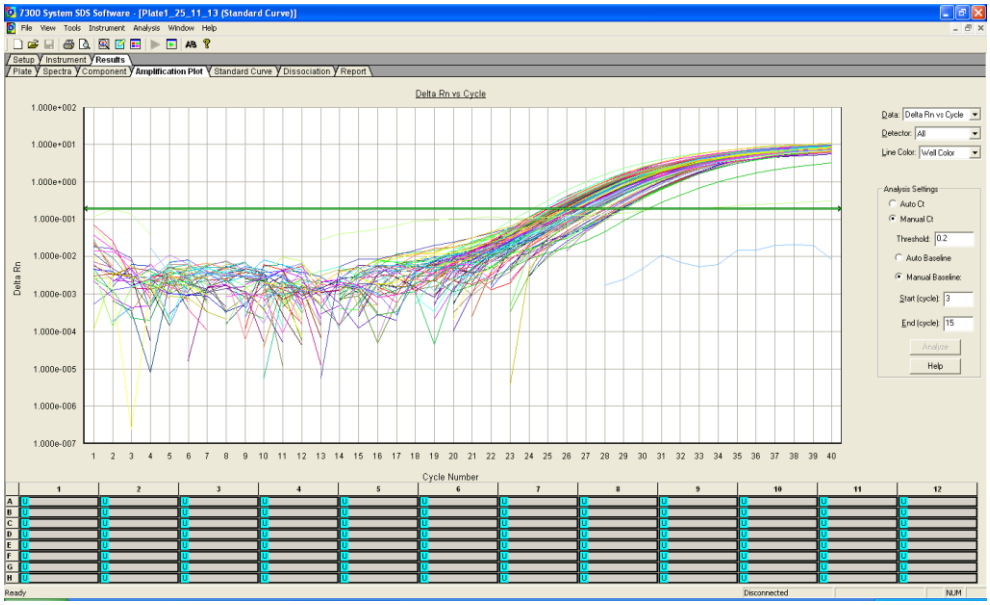

Fig. 4 *qPCR screen print*

Data outcome is threshold cycles (C_t) and is a log-linear plot of PCR signal *vs*. cycle number.
Low C_t equals high level of cDNA since threshold is reached faster.

Threshold is an arbitrary value set by the computer.

Immunohistochemistry

As previously mentioned, reverse transcriptase qPCR only verifies the presence of mRNA which does not necessarily proves expression of the proteins. For this matter, immunohistochemistry is a useful technique where specific antibodies are used to track gene expression at protein level. Several methods are available where proteins are detected from tissue preparations and isolated cells (Strachan and Read 2011). In the present study previously tested antibodies (Li, Timofeyev et al. 2009) were used to obtain an overall expression pattern of SK2 and SK3 within the cardiac tissue. The mechanism behind immunohistochemistry is simple antigen-antibody binding, visualized by fluorescence microscopy. The term ‘antigen’ is usually referred to invading, non-self microorganisms or toxins but in the case of immunohistochemistry ‘antigen’ is used for all kind of proteins and, in this study, describes the entire ion channel. Epitope on the other hand is a term used to describe only the actual molecular structure of the antigen interacting with the antibody (Ab). Antibodies are immunoglobulins (Ig) designed to target one specific epitope. Antibodies are usually harvested from animals which have been repeatedly exposed to the antigen of interest and so have initiated an immune response. This *in vivo* process results in antibodies produced from several different B lymphocytes each of which targeting different epitopes of the antigen. Antibodies obtained this way are therefor known as polyclonal antibodies. If a homogeneous batch of antibodies is desired, single B lymphocyte producing specific antibodies can be cloned into an immortal cell line (e.g. tumor cells). This provides a stable source of Ab’s all targeting the same epitope and is therefore termed monoclonal antibodies (Strachan and Read 2011). To visually locate

the proteins, a fluorophore are bound to the antibody and the light can be detected by a fluorescence microscope. If the fluorophore is bound directly to the Ab targeting the protein the method is termed direct immunofluorescence. However, indirect immunofluorescence where a secondary antibody is included is more commonly used. The principle is simple: The primary antibodies is mounted on the tissue and will only bind to the specific epitope of the antigen. The tissue is washed and all excess Ab is removed. The primary Ab contains a specific binding site itself and functions as an antigen to the secondary antibody which has the fluorophore attached (Fig.5). Secondary antibodies can be purchased with fluorophores having different wavelength thus allowing co-staining (Fritschy 2008).

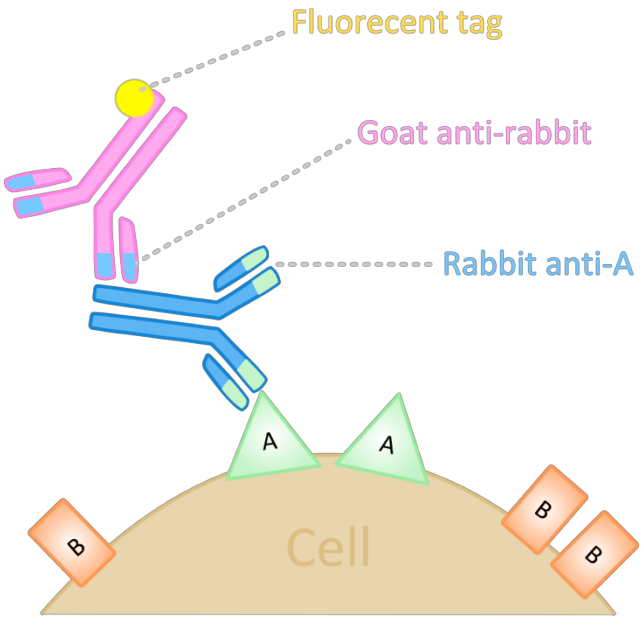

Fig. 5 *Schematic illustration of indirect immunofluorescence*. The primary AB (blue) binds to the antigen (A) and the secondary AB with the fluorescent tag (pink) binds to the primary AB.

It is important that both the primary and secondary antibodies are very specific and only binds to the ion channel in question. First of all the complementary amino acid (AA) sequence of the antibody should only match the epitope of the ion channel of interest. The specificity of an antibody can be tested by a protein BLAST (basic local alignment search tool) which is an online software program found at NCBI's webpage. The program compares an entered AA sequence to, in this case, all known AA sequences of the equine genome. Secondly, it should be tested whether the antibody has more than one binding site. This can be tested by incubating the primary antibody with a

peptide matching the AA sequence prior to hybridization. If the antibody is specific the peptide will occupy all binding sites and the primary antibody will be washed away thus leaving no signal. To ensure that there is no unspecific binding from the secondary antibody an experiment where the primary antibody is left out, should be performed. The two controls are in this paper named 'peptide control' and '2nd control' respectively. It should be emphasized that both the actual experiments and the controls need to be done at the same time since even small variations can have great consequences (Fritschy 2008).

Ideally, two additional controls should have been included in this study; a positive and a negative control. A positive control is often tissue known to have a high expression of the epitope of interest (natural occurring or transfected) where the negative control is tissue lacking the target antigen (e.g. knockout mouse) (Hsi 2001). Due to the short period of time giving to this project these experiments were not possible to perform. However, other research groups have previously confirmed the validity of the SK2 antibodies in knockout mice (Li, Timofeyev et al. 2009).

The frozen blocks of equine atrial and ventricular trabecular muscles were embedded in Tissue-Tek® medium (Sakura Fintak, Netherlands) and then cut in 12 µm slices on a cryostat setup (Leica CM3050S, Leica Microsystems, Germany). The slices were mounted on positively charged Superfrost® Plus microscope slides (Thermo Scientific, Germany) and stored at room temperature until usage. The chosen antibodies have previously been tested on human tissue and only few optimizing adjustments were made to the protocol. First, the cryosections were rehydrated in a phosphate buffered saline (PBS) solution and later fixated in 4% paraformaldehyde (made in PBS). They were blocked in PBS containing 4% bovine serum albumin (to reduce background staining) and 0.2% Triton X-100 (to perforate the membrane). The primary antibodies were mounted on the slices and incubated at 4°C overnight. The slices were washed repeatedly in PBS and incubated with fluorochrome-coupled secondary antibodies for one hour at room temperature. After additional washes the sections were mounted in ProLong Gold® (Invitrogen) mounting medium.

Three different primary SK antibodies were tested and their properties are shown below (table 2). Data for one experiment (Anti-KCNN2, Sigma-Aldrich) is left out as the peptide was not available and the necessary controls could therefore not be performed. We co-stained with anti-connexin 43 to visualize the intercalated discs (Beyer, Paul et al. 1987) and with DAPI which is a small molecule with strong affinity to DNA that becomes fluorescent when bound, resulting in strong staining of the nucleus (Kapuscinski 1995) (Table 2).

Name	Manufacturer	Host	Type	Sequence	Concentration
Anti-K_{Ca}2.2 (SK2)	Alomone	Rabbit	Primary, Polyclonal	CETQMENYDKH VTYNAERS	1:200
Anti-K_{Ca}2.3 (SK3)	Alomone	Rabbit	Primary, Polyclonal	DTSGHFHDSGV GDLDEDPKC	1:200
Anti-KCNN2 (SK2)	Sigma-Aldrich	Rabbit	Primary, Polyclonal	KNAAANVLRETWLIYKN TKLVKKIDHAKVRKHQR FFLQAIHQLRSVKMEQ	1:200
Anti-Connexin43	Invitrogen	Mouse	Monoclonal	Not available	1:200
AlexaFluor®568	Life Technologies	Goat	Secondary	Anti-rabbit	1:200
AlexaFluor®488	Life Technologies	Goat	Secondary	Anti-mouse	1:200
DAPI	Invitrogen		4′,6-diamidino-2-phenylindole		1:300

Table 2 *Properties of AB*. Primary and secondary AB used to stain for SK channels, connexin43 and nucleus

Stained slices of cardiomyocytes from right atria and right ventricle was evaluated using a Zeiss 710 confocal microscope (Carl Zeiss Microscopy GmnH, Germany). This laser scanning microscope (LSM) is a complex machine capable of detecting light from the fluorophore. Light from a laser is sent through an excitations filter (also known as the collimator) and the beam splitter that only allows light of a specific wavelength to pass. The light is reflected through the objective lens and focused on the tissue. Here, the fluorophores absorbs the light and reflect back light of a different wavelength also called emission light. The emission light passes through the beam splitter and the emission filter and is detected by the computer. According to the fluorophores attached to the secondary antibodies the laser, the excitations filter, the beam splitter and emissions filter is carefully chosen and the emission light is detected one by one. The confocal LSM has an extra element compared to conventional microscopes; the confocal aperture usually called pinhole. It obstructs all light outside the focal plane only detecting the in-focus light. This allows precise thin optical imaging from "thick" biological slices (Wilhelm). When imaging, identical microscope and laser settings was used for sample and controls but differed between atria and ventricles and the two antibodies. A schematic illustration of the confocal LSM is presented in figure 6.

Detailed protocols for all the experiments are found in appendix A.

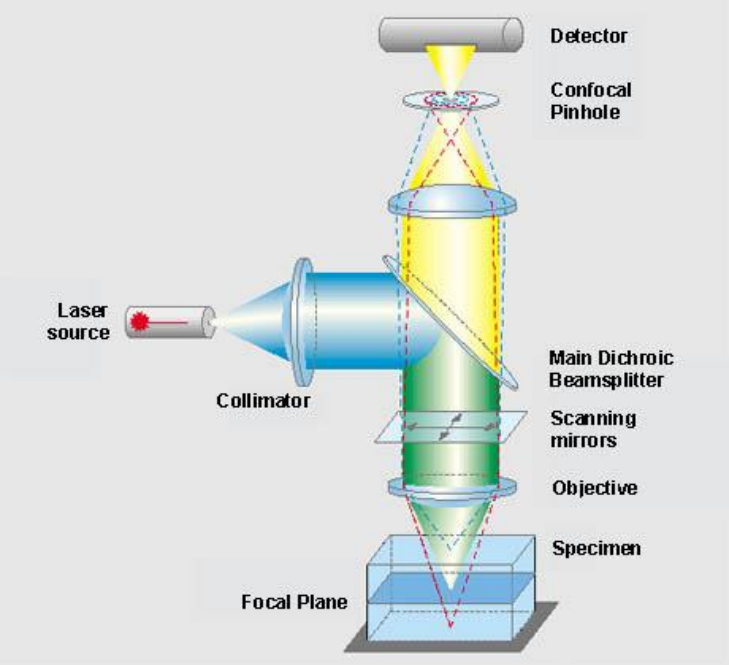

Fig. 6 *Schematic illustration of the confocal laser scanning microscope*. Light from the laser is sent through the collimator, beam splitter and focused on the tissue. The fluorophores absorbs the light and reflect back emission light. The pinhole only allows light from the focal plane to be detected. Figure adapted from www.ziess.de

Statistical analysis

qPCR data was retrieved by SDS1.2 software (Applied Biosystems, USA) and was imported to excel spread sheet. Statistical analyses were carried out using Prism 5.01 (GraphPad, San Diego, California, USA). Differences in expression level between atria and ventricles were evaluated by unpaired *t*-test. Differences in expression level with in the left ventricle (LV Endo, LV Mid, LV Epi) were assessed using a One-Way ANOVA test followed by a Bonferroni multiple comparisons post-test. All data were attempted tested for Gaussain distribution using D'Agostino&Pearson omnibus normality test, however n were too small. From this, non-parametric tests such as Mann-Whitney and Kruskall-Wallis test would probably have been more correct to use. However, to be able to compare our results with previously published data the common *t*-test and ANOVA test was chosen. A 5% significance level was used and indicated by asterisks; * = $P<0.05$, ** = $P<0.01$, *** = $P<0.001$. Results are expressed as mean ± SEM.

Results

Equine tissue samples

All horses were visually inspected prior to slaughter. Six horses were auscultated and four had a brief (1-2 minutes) ECG recorded. No murmurs or arrhythmia was detected. Following mRNA isolation, five of 11 samples did not present with clear bands on the agarose gel and were therefore

excluded (Fig. 7). This was probably the result of the less than optimal tissue harvest. The slaughter of the horses was very effective but the tissue harvest was very time-comsuming and some hearts were left non-preserved for several hours.

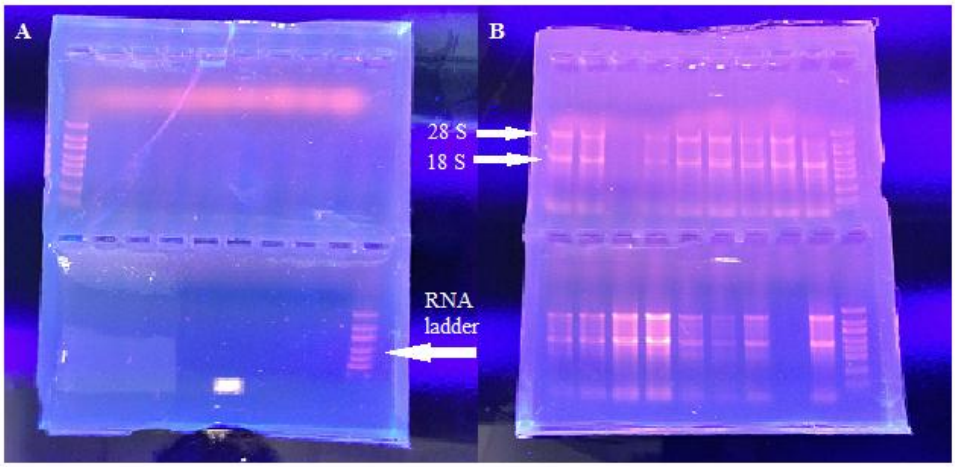

Fig. 7 *RNA quality validation on agarose gel*

Five of 11 horses did not present with clear bands of 28 S or 18 S ribosomal RNA (A).
The remaining six horses did present with clear bands of 28 S and 18 S ribosomal RNA and were included in the following experiments.

An overview of the relative expression profile for the 14 genes investigated is provided in Table 3. Exact values are found in appendix A.

	RA		LA		RV		LV Endo		LV Mid		LV Epi	
	Mean	SEM	Mean	SEM	Mean	SEM	Mean	SEM	Mean	SEM	Mean	SEM
SCN5A	11.94	4.7	8.70	1.1	9.53	2.5	8.54	1.8	11.23	2.4	17.11	8.0
KCNH2	0.37	0.1	0.32	0.1	2.99	0.8	2.23	0.5	3.15	0.6	4.42	2.3
KCNQ1	8.53	2.7	8.42	2.4	14.61	2.2	11.50	4.0	10.89	1.5	18.29	7.4
KCNA5	12.58	4.1	9.41	2.7	5.84	2.0	4.14	2.0	2.94	0.9	3.08	1.1
KCNJ3	22.80	5.0	19.31	5.3	8.21	4.3	5.46	0.7	12.12	2.9	14.88	7.1
KCNJ5	82.10	31.0	64.24	15.63	4.08	3.5	0.29	0.1	3.33	2.7	0.39	0.1
KCNN1	2.38	0.8	1.68	0.3	4.72	3.2	1.67	0.3	2.10	0.3	1.46	0.3
KCNN2	0.49	0.3	2.29	1.3	0.19	0.1	0.19	0.04	0.30	0.1	0.42	0.2
KCNN3	4.97	2.0	6.34	2.4	7.06	3.8	2.91	0.9	2.76	0.4	4.15	1.5
KCNJ2	2.96	0.9	2.44	0.6	54.02	14.3	30.73	7.4	45.10	9.8	72.96	35.6
KCNIP2	19.37	4.5	5.52	0.9	43.09	15.8	32.50	10.3	31.68	9.3	29.02	6.7
KCND3	22.05	6.3	21.29	4.3	34.36	13.4	18.19	3.5	21.65	3.3	26.62	10.3
CACNA1C	22.00	6.1	17.22	3.4	38.00	7.9	30.72	5.5	42.82	6.2	59.98	24.1
ACTB	22.01	0.3	22.14	0.5	23.25	0.6	23.10	0.5	22.96	0.1	22.87	0.4

Table 3 *Normalized data from real-time PCR with beta-actin (ACTB) as reference gene*. Units for all expression values are $100 * 2^{-\Delta Ct}$. Abbreviations: RA: right atrium, LA: left atrium, RV: right ventricle, LV Endo: left ventricular endocardium, LV Mid: left ventricular midmyocardium, LV Epi: left ventricular epicardium

mRNA analysis

The voltage-gated sodium channel Nav1.5 (SCNA5) was equally expressed in both atria and ventricles. ERG1, the ion channel responsible for I_{Kr} (KCNH2) were overall expressed at low levels but predominated the ventricles ($P = 0.0073$). There was no significant difference in the expression level between atria and ventricles for KCNQ1 and KCNA5, the genes encoding the slow (Kv7.1) and ultra-rapid (Kv1.5) rectifying current respectively. There is, however, a small tendency for KCNA5 to dominate the atria which are also the case for KCNJ3 (Kir3.1). KCNJ5, the gene responsible for the other acetylcholine-depended (I_{KAch}) current (Kir3.4) showed a markedly increased expression level in the atria compared to the ventricles ($P = 0.0312$). The transcript of KCNJ2 (Kir2.1, responsible for I_{K1}) predominated the ventricles significantly ($P = 0.0051$). KCNIP2 (KChiP2, Ca^{2+}-sensitive Kv channel-interacting protein) had a tendency to be more expressed in the ventricles than the atria. Kv4.3, the channel of the fast transient outward potassium current I_{to} encoded by KCND3 also tends to have higher transcript level in the ventricles. The L-type Ca^{2+}-channel Cav1.2 (CACNA1C) were present in all heart regions but with a tendency to dominate the ventricles. There were no significant differences in the transmural expression across the left ventricle for any of the genes. The transcriptional expression in the right atria vs. right ventricle of the above mentioned genes are depicted in Fig. 8A.

Transcripts of all three isoforms of the SK channels (SK_{Ca}) were present in the horse heart. SK1 and SK3 were highly expressed in all regions of the heart, and SK3 was the most prominent of all three isoforms. Although no significant difference was demonstrated, SK2 showed a tendency to increased expression in the left atria, slightly less in the right atria and low levels in the ventricles. Distribution of SK1, SK2 and SK3 are visualized in Fig. 8 B+C.

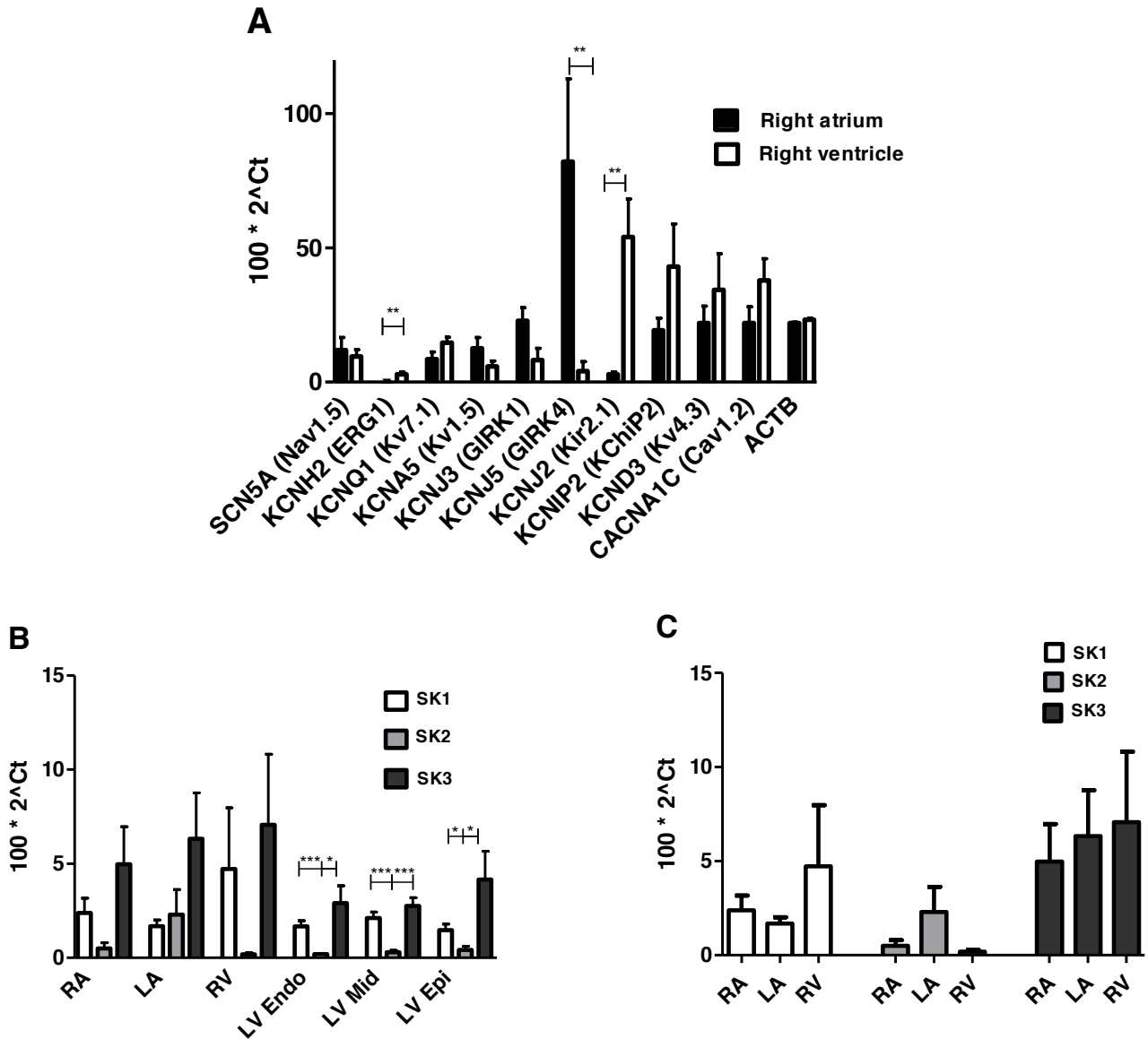

Fig. 8 *Expression profile by real-time PCR of Na^+, Ca^{2+} and K^+ channel subunits in the equine heart*. **A**: Comparison of right atrium *vs*. right ventricle. **B**: Relative distribution of the three isoforms of SK channels in the right atrium, left atrium, right ventricle and left ventricular endo-, mid and epicardium. **C**: Relative distribution of SK1, SK2 and SK3 in RA, LA and RV.

Immunohistochemistry and confocal microscopy

The antibodies available were directed against epitopes of human SK proteins so a BLAST was performed initially. The amino acid sequence of Anti-K_{Ca}2.2 (SK2) (Alomone) was 94% (17/18 AA) identical to the equine SK2 channel protein and Anti-K_{Ca}2.3 (SK3) (Alomone) was 100% (20/20 AA) identical to the equine SK3 channel protein, why we proceeded with the experiments. The AA sequence of Anti-KCNN2 (Sigma-Aldrich) was 98% (49/50) identical with equine SK2,

94% (47/50 AA) with equine SK3 and 83% (44/50) with equine SK1. The specific peptide however, was not available and no control experiments could be performed. Hence, the Anti-KCNN2 results are not presented.

Immunolocalization of both SK2 and SK3 proteins was performed on 12 µm thick slices of tissue from the right atrium and the right ventricle, respectively. SK2 antibody staining revealed a widespread distribution of SK2 channels in both atrial and ventricular cells. SK2 were primary located in the periphery of the cells but also in a striated pattern across the cell. SK2 staining with antigen included or with only secondary AB showed no visible staining. Staining with SK3 antibody showed similar patterns, however the intensity of the staining was more pronounced. This was due to unspecific staining revealed by the controls (Fig. 9-11).

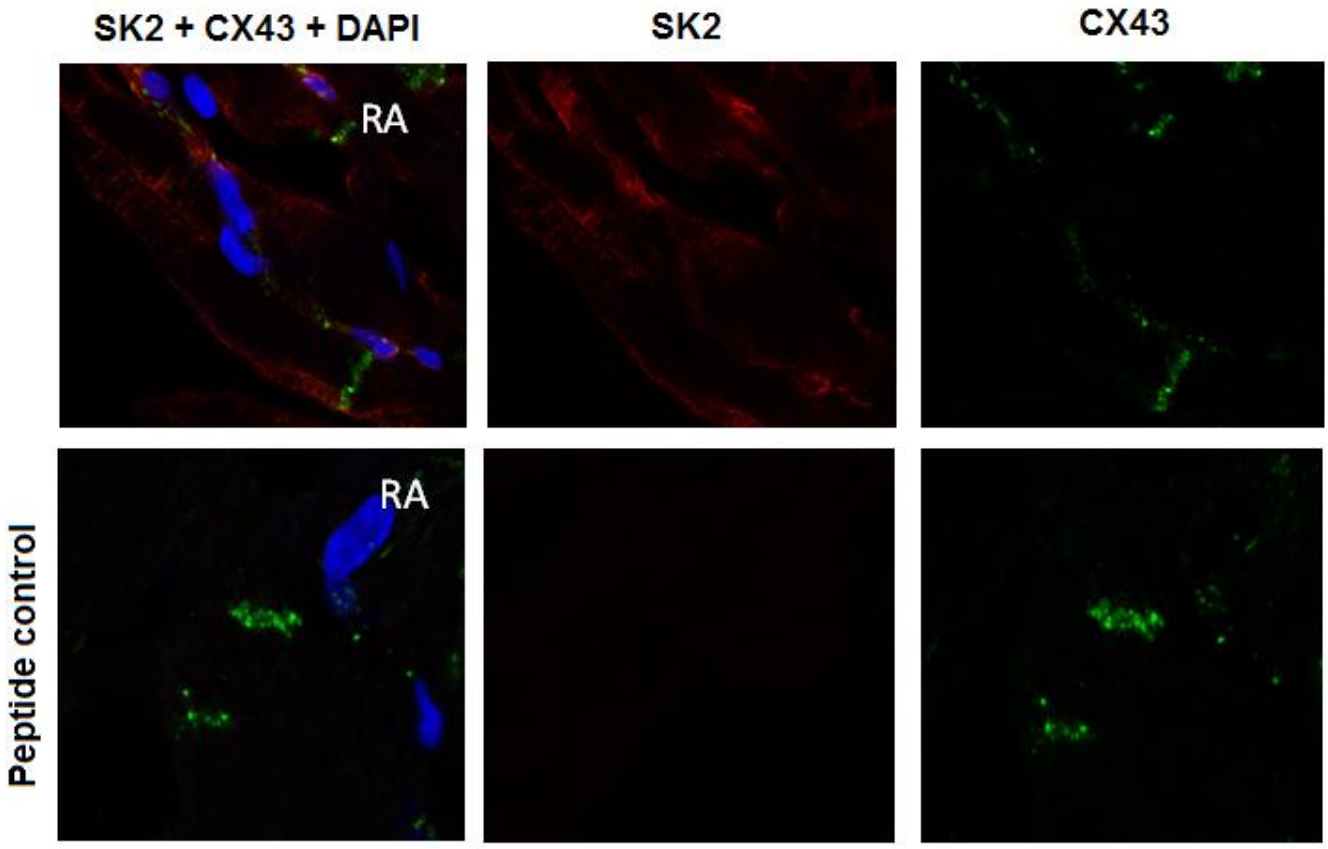

Fig. 9 *Immunohistochemistry of equine right atrium*. 1:200 SK2 antibody (red), 1:200 connexin 43 (green) and 1:300 DAPI antibody (blue). SK2 staining reveals widespread distribution of SK2 channels in both the periphery of the cell and in a striated pattern across the cell.
Both peptide control and the control only containing the secondary AB showed no visible staining.
Only the peptide control is presented. Light intensity of all images is increased by 30%.

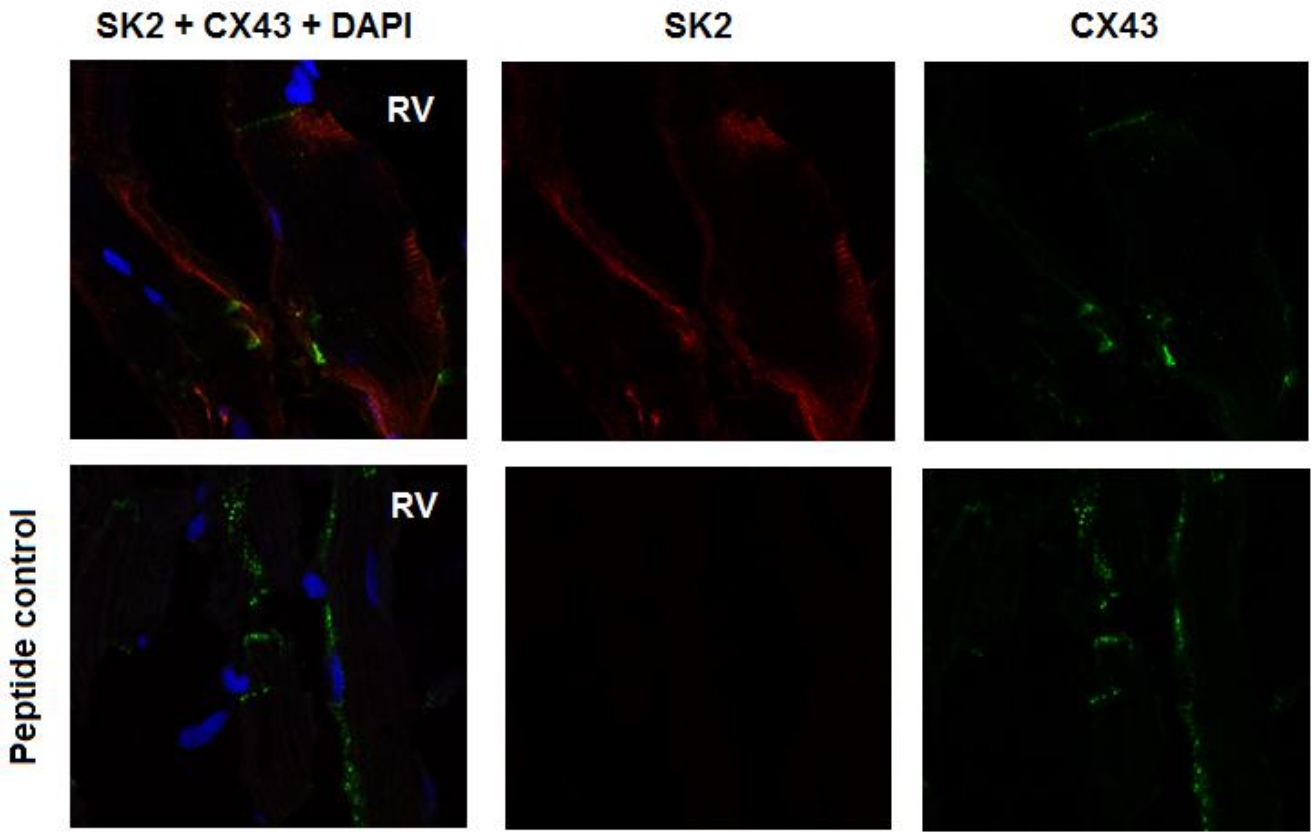

Fig. 10 *Immunohistochemistry of equine right ventricle*. 1:200 SK2 antibody (red), 1:200 connexin 43 (green) and 1:300 DAPI antibody (blue). Similar to the atrium SK2 channels are present in the ventricle. Imaging settings are not identical why no quantitative comparison can be made. Both controls showed no visible staining. Only the peptide control is presented. Light intensity of all images is increased by 30%.

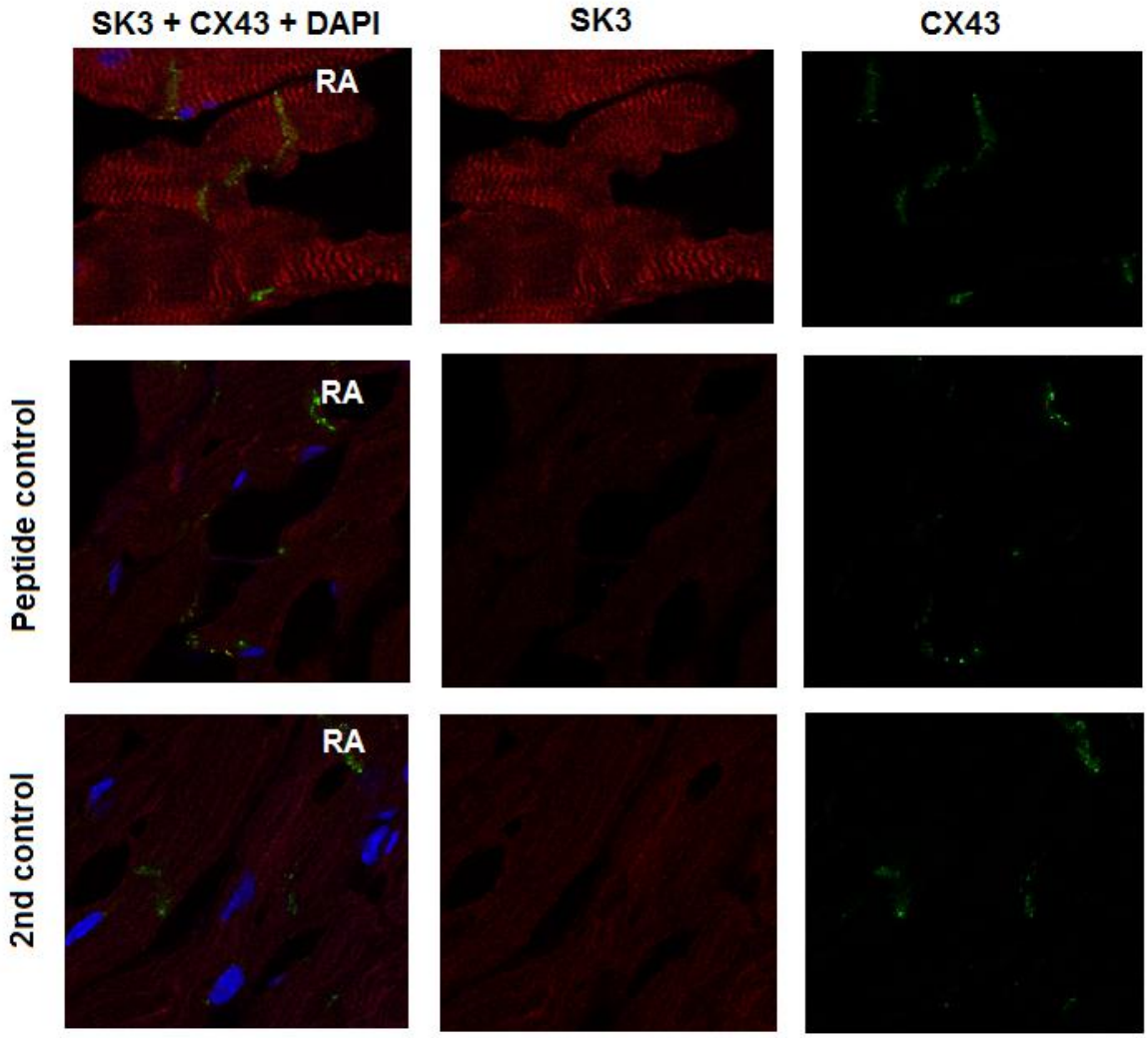

Fig. 11 *Immunohistochemistry for equine right atrium*. 1:200 SK3 antibody (red), 1:200 connexin 43 (green) and 1:300 DAPI antibody (blue). Staining with SK3 anti-body reveals strong staining of SK3 channels. However, both controls also present with staining why the specificity of the AB should be questioned. Light intensity of all images is increased by 30%

Discussion

Gene expression

This study is the first to characterize the distribution of the most important ion channels in the equine heart. qPCR permits comparison of the relative expression level among genes. With a few variations, the gene expression pattern of the equine cardiac ion channels is very similar to the gene expression documented in the human heart (Gaborit, Le Bouter et al. 2007). The differences and their possible effects on the action potential are discussed below. One of the variances seen is expression level of Kv1.5, responsible for the I_{Kur} current. It has predominantly been reported as aria specific with at 45 fold higher expression compared to the ventricles (Nerbonne and Kass 2005), (Gaborit, Le Bouter et al. 2007). In the horse, Kv1.5 is expressed in both atria and ventricles with only a tendency towards more pronounced expression in the atria. Transcript of Kv1.5 in the ventricles have also been demonstrated in the Göttingen minipig (Laursen, Olesen et al. 2011) and lately in canine and human ventricular tissue (Calloe, Soltysinska et al. 2010). In both studies KCNA5 is expressed more in the atria that in the ventricles, consistent with previously results. I_{to} and I_{Kur} are believed to cause the rapid repolarization seen in the atria compared to the ventricles (Nerbonne and Kass 2005). Both these currents are, at least at mRNA level, presence in the equine ventricle. The effect on the shape of the action potential could be interesting to study. Only one study, recording an AP in isolated myocytes from the equine ventricular epicardium has been published and the result can be seen in figure 12. (Finley, Li et al. 2002).

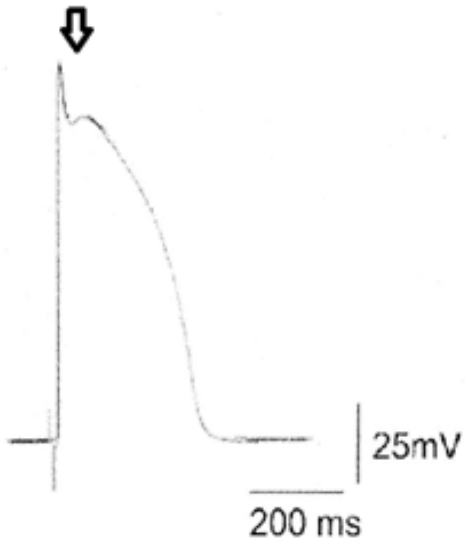

Fig. 12 *AP recorded from equine ventricular epicardium*. The notch (arrow) could be due to the I_{to} and I_{Kur} currents. The figure is modified from (Finley, Li et al. 2002)

The notch seen on the AP (arrow) could be the I_{Kur} current producing a partly rapid repolarization together with I_{to}. Kv1.5 has been suggested to have therapeutic value for AF due to the strong expression in the atria (Dobrev, Carlsson et al. 2012). The expression of Kv1.5 in the ventricles proposes a potential risk of ventricular proarrhythmia when blocking Kv1.5 in the horse. However, before any conclusions can be made, the functionally effect of Kv1.5 in the ventricles should be thoroughly investigated.

ERG1 had an overall low expression level, however, the expression was significantly more in the ventricles than atria. This differs from human literature where HERG1 has a uniform and high expression level (Gaborit, Le Bouter et al. 2007). One other study has investigated ERG1 and KCNQ1 in the equine heart (Finley, Li et al. 2002). They demonstrated the presence of the ion channels encode by ERG1 and KCNQ1 in both atria and ventricles but no quantitative methods were used. Similar to our findings ERG1 has a tendency to dominate the ventricle in the Göttingen minipig (Laursen, Olesen et al. 2011).

By characterization of the major cardiac ion channels expressed in the horse we have provided a solid foundation from where future research can progress. We have furthermore demonstrated the resemblance between the human and equine ion channel expression profile and therefore suggest that equine hearts can constitute a *bona fida* model of human AF.

Immunohistochemistry

Human Anti-$K_{Ca}2.2$ (SK2) (Alomone) antibodies have been proven useful in staining for SK2 channels in equine cardiac tissue. Anti-$K_{Ca}2.3$ (SK3) (Alomone) antibodies revealed unspecific binding by staining both the controls. Only the primary antibody differed in the two experiments and in the 2nd control experiments the primary antibody was left out. Yet, the SK3 2nd control was stained by the secondary antibody while the SK2 2nd control was not. The SK3 protocol could be optimized by altering the concentration of secondary antibody. However, with the amount of unspecific staining revealed by the peptide control the specificity of the primary antibody is doubtful. The result of the BLAST of Anti-KCNN2 (Sigma-Aldrich) showed affinity for all isoforms of the SK channels why this antibody could be interesting to test with the proper controls. The advantage of immunohistochemistry is, unlike qPCR, that you detect the translated protein and not just the DNA or mRNA. However, there are several pitfalls of this method that is important to bear in mind when interpreting the staining. Immunohistochemistry highly relies on the specificity

of the antibodies. Both false-positive and, equally important, false-negative results is a consequence of unspecific staining (Fritschy 2008). In this study neither a positive control nor a negative knockout control was included why the results should be interpreted carefully. Furthermore, the tissue quality varied which can lead to false-negative findings. Quantification should only be attempted when the exact same settings have been applied in all experiments. This is not the case in this study why the results should only be interpreted in a qualitative manner. Although there are some limitations to this study the findings from the immunohistochemistry is supported by the qPCR and the *in vivo* experiments where horses converted from AF to sinus rhythm after treatment with an SK modulator.

SK channel expression in the equine heart

Several studies claim that the SK channels are atrial specific and therefore exhibit as a good candidate for novel drug therapy, terminating AF (Xu, Tuteja et al. 2003), (Nattel 2009), (Yu, Deng et al. 2012). In this study, results from the qPCR showed that mRNA from SK1, SK2 and SK3 are present both in atria and ventricles. SK3 showed highest transcript level with uniform distribution in RA, LA and RV. Slightly less was found in the left ventricle. SK1 was primarily found in RV but was present in all the investigated locations of the heart. SK2 showed an overall low expression but tended to predominate the left atria. Staining with SK2 specific antibody equally verified the presence of SK2 channels in both atria and ventricles. To this date no other studies investigating SK channel expression in the equine heart have been published, why no comparisons can be made. The inconsistency in our finding compared to previously human studies claiming that SK_{Ca} is atria specific could be species dependent. However, in this study we found that the general ion channel distribution of the equine heart largely resembles the human ion channel expression profile, why this should be questioned. Furthermore, studies using qPCR to quantify the SK1-3 expression in mice (Tuteja, Xu et al. 2005) and dogs (Qi, Diness et al. 2014) also found SK expression in both atria and ventricles. Most papers claiming the atrial specificity of the SK channels are referring to the work done by Xu and coworkers (2003). Using the patch clamp technique and the SK blocker apamin they demonstrated a prolongation of the action potential. The prolongation of the AP was markedly pronounced in the atria compared to the ventricles. Their argument was further supported by western blot and RT PCR. The outcomes of both these methods are evaluated visually, which makes is a subjective evaluation that are not suited for quantification. The patch clamp results however, have been reproduced several times (Tuteja, Xu et al. 2005), (Diness, Sorensen et al.

2010). It should be noted that SK2 is the SK subtype most sensitive to apamin (Xu, Tuteja et al. 2003) and will be the one primary affected when apamin is applied. This is consistent with our findings where SK2 predominates the atria. It is therefore likely to assume that SK channels are somewhat atria specific functionally but not in mRNA expression. However, further studies need to done before any final conclusions can be made.

Conclusion

In the present study we have characterized the expression level and distribution of the most prominent calcium, sodium and potassium ion channels in the equine heart (Cav1.2, Nav1.5, Kv4.3, KChiP2, Kv1.5, ERG1, Kv7.1, Kir2.1, GIRK1 and GIRK4). We have demonstrated that the expression pattern to a large extend resembles the human expression profile. The variation between horses and humans includes; expression of Kv1.5 (KCN5A) in both atria and ventricles and an overall low expression of ERG (Kv11.1) in the equine heart. In addition, we have verified the presences of the three isoforms of the cardiac small-conductance Ca^{2+}-activated potassium channels (SK1, SK2 and SK3) in the horse. Our results suggest that equine hearts may constitute a *bona fida* model of human arrhythmias.

Perspectives

The research presented in this study has provided a solid foundation in understanding the equine cardiac electrophysiology from where future research can expand.

As previously mentioned, reverse transcriptase qPCR only verifies the presence of mRNA. To further validate our findings western blot could be performed on all ion channels to characterize their expression on protein level. Furthermore, it is desirable to validate the presence of the SK channels with a positive control and negative knockout control in the immunohistochemistry experiments.

However, to obtain full knowledge of the equine cardiac electrophysiology, if ever possible, several further experiments are required. First of all, the AP is modulated by a several ion currents not included in this study and their expression profile needs to be characterized. Then the functional role of the ion channels and their effect on the AP should be determined. The different current's effect on the AP can be analyzed using microelectrode recordings and whole cell patch-clamp

analysis combined with antagonists of the different ion channels. The equine expression profile of KCNA5 (I_{Kur}) differed from humans and it would be very interesting to analyze the effect of I_{Kur} on the equine ventricular AP.

Finally, a thorough investigation of the ion channel expression profile and AP modulation in horses with AF would provide great knowledge useful in AF treatment.

References

An, W. F., M. R. Bowlby, M. Betty, J. Cao, H. P. Ling, G. Mendoza, J. W. Hinson, K. I. Mattsson, B. W. Strassle, J. S. Trimmer and K. J. Rhodes (2000). "Modulation of A-type potassium channels by a family of calcium sensors." Nature **403**(6769): 553-556.

Barbesgaard, L., R. Buhl and C. Meldgaard (2010). "Prevalence of exercise-associated arrhythmias in normal performing dressage horses." Equine Vet J Suppl(38): 202-207.

Bean, B. P. (1985). "Two kinds of calcium channels in canine atrial cells. Differences in kinetics, selectivity, and pharmacology." J Gen Physiol **86**(1): 1-30.

Beyer, E. C., D. L. Paul and D. A. Goodenough (1987). "Connexin43: a protein from rat heart homologous to a gap junction protein from liver." J Cell Biol **105**(6 Pt 1): 2621-2629.

Bustin, S. A. and T. Nolan (2004). "Pitfalls of quantitative real-time reverse-transcription polymerase chain reaction." J Biomol Tech **15**(3): 155-166.

Calloe, K., E. Soltysinska, T. Jespersen, A. Lundby, C. Antzelevitch, S. P. Olesen and J. M. Cordeiro (2010). "Differential effects of the transient outward K(+) current activator NS5806 in the canine left ventricle." J Mol Cell Cardiol **48**(1): 191-200.

Chen, M. X., S. A. Gorman, B. Benson, K. Singh, J. P. Hieble, M. C. Michel, S. N. Tate and D. J. Trezise (2004). "Small and intermediate conductance Ca(2+)-activated K+ channels confer distinctive patterns of distribution in human tissues and differential cellular localisation in the colon and corpus cavernosum." Naunyn Schmiedebergs Arch Pharmacol **369**(6): 602-615.

Chomczynski, P. and N. Sacchi (2006). "The single-step method of RNA isolation by acid guanidinium thiocyanate-phenol-chloroform extraction: twenty-something years on." Nat Protoc **1**(2): 581-585.

Diness, J. G., U. S. Sorensen, J. D. Nissen, B. Al-Shahib, T. Jespersen, M. Grunnet and R. S. Hansen (2010). "Inhibition of small-conductance Ca2+-activated K+ channels terminates and protects against atrial fibrillation." Circ Arrhythm Electrophysiol **3**(4): 380-390.

Dobrev, D., L. Carlsson and S. Nattel (2012). "Novel molecular targets for atrial fibrillation therapy." Nat Rev Drug Discov **11**(4): 275-291.

Finley, M. R., Y. Li, F. Hua, J. Lillich, K. E. Mitchell, S. Ganta, R. F. Gilmour, Jr. and L. C. Freeman (2002). "Expression and coassociation of ERG1, KCNQ1, and KCNE1 potassium channel proteins in horse heart." Am J Physiol Heart Circ Physiol **283**(1): H126-138.

Fritschy, J. M. (2008). "Is my antibody-staining specific? How to deal with pitfalls of immunohistochemistry." Eur J Neurosci **28**(12): 2365-2370.

Gaborit, N., S. Le Bouter, V. Szuts, A. Varro, D. Escande, S. Nattel and S. Demolombe (2007). "Regional and tissue specific transcript signatures of ion channel genes in the non-diseased human heart." J Physiol **582**(Pt 2): 675-693.

Holmes, J. R., M. Henigan, R. B. Williams and D. H. Witherington (1986). "Paroxysmal atrial fibrillation in racehorses." Equine Vet J **18**(1): 37-42.

Hsi, E. D. (2001). "A practical approach for evaluating new antibodies in the clinical immunohistochemistry laboratory." Arch Pathol Lab Med **125**(2): 289-294.

Kapuscinski, J. (1995). "DAPI: a DNA-specific fluorescent probe." Biotech Histochem **70**(5): 220-233.

Laursen, M., S. P. Olesen, M. Grunnet, T. Mow and T. Jespersen (2011). "Characterization of cardiac repolarization in the Gottingen minipig." J Pharmacol Toxicol Methods **63**(2): 186-195.

Leroux, A. A., J. Detilleux, C. F. Sandersen, L. Borde, R. M. Houben, A. Al Haidar, T. Art and H. Amory (2013). "Prevalence and risk factors for cardiac diseases in a hospital-based population of 3,434 horses (1994-2011)." J Vet Intern Med **27**(6): 1563-1570.

Li, N., V. Timofeyev, D. Tuteja, D. Xu, L. Lu, Q. Zhang, Z. Zhang, A. Singapuri, T. R. Albert, A. V. Rajagopal, C. T. Bond, M. Periasamy, J. Adelman and N. Chiamvimonvat (2009). "Ablation of a Ca2+-activated K+ channel (SK2 channel) results in action potential prolongation in atrial myocytes and atrial fibrillation." J Physiol **587**(Pt 5): 1087-1100.

Livak, K. J. and T. D. Schmittgen (2001). "Analysis of relative gene expression data using real-time quantitative PCR and the 2(-Delta Delta C(T)) Method." Methods **25**(4): 402-408.

Marr, C. and M. Brown (2010). Cardiology of the Horse, Saunders Elsevier.

Nattel, S. (2009). "Calcium-activated potassium current: a novel ion channel candidate in atrial fibrillation." J Physiol **587**(Pt 7): 1385-1386.

Nerbonne, J. M. and R. S. Kass (2005). "Molecular physiology of cardiac repolarization." Physiol Rev **85**(4): 1205-1253.

Ohmura, H., A. Hiraga, T. Takahashi, M. Kai and J. H. Jones (2003). "Risk factors for atrial fibrillation during racing in slow-finishing horses." J Am Vet Med Assoc **223**(1): 84-88.

Petitprez, S., T. Jespersen, E. Pruvot, D. I. Keller, C. Corbaz, J. Schlapfer, H. Abriel and J. P. Kucera (2008). "Analyses of a novel SCN5A mutation (C1850S): conduction vs. repolarization disorder hypotheses in the Brugada syndrome." Cardiovasc Res **78**(3): 494-504.

Qi, X. Y., J. G. Diness, B. J. Brundel, X. B. Zhou, P. Naud, C. T. Wu, H. Huang, M. Harada, M. Aflaki, D. Dobrev, M. Grunnet and S. Nattel (2014). "Role of small-conductance calcium-activated potassium channels in atrial electrophysiology and fibrillation in the dog." Circulation **129**(4): 430-440.

Ravens, U. (2010). "Antiarrhythmic therapy in atrial fibrillation." Pharmacol Ther **128**(1): 129-145.

Sanguinetti, M. C. and N. K. Jurkiewicz (1992). "Role of external Ca2+ and K+ in gating of cardiac delayed rectifier K+ currents." Pflugers Arch **420**(2): 180-186.

Singer, V. L., T. E. Lawlor and S. Yue (1999). "Comparison of SYBR Green I nucleic acid gel stain mutagenicity and ethidium bromide mutagenicity in the Salmonella/mammalian microsome reverse mutation assay (Ames test)." Mutat Res **439**(1): 37-47.

Strachan, T. and A. Read (2011). Human Molecular Genetics, Garland Sciences.

Trudeau, M. C., J. W. Warmke, B. Ganetzky and G. A. Robertson (1995). "HERG, a human inward rectifier in the voltage-gated potassium channel family." Science **269**(5220): 92-95.

Tuteja, D., D. Y. Xu, V. Timofeyev, L. Lu, D. Sharma, Z. Zhang, Y. F. Xu, L. P. Nie, A. E. Vazquez, J. N. Young, K. A. Glatter and N. Chiamvimonvat (2005). "Differential expression of small-conductance Ca2+-activated K+ channels SK1, SK2, and SK3 in mouse atrial and ventricular myocytes." American Journal of Physiology-Heart and Circulatory Physiology **289**(6): H2714-H2723.

Wilhelm, S., Gröbler, B., Gluch, M. and Heinz, H. Confocal laser scanning microscopy principles.

Xu, Y., D. Tuteja, Z. Zhang, D. Xu, Y. Zhang, J. Rodriguez, L. Nie, H. R. Tuxson, J. N. Young, K. A. Glatter, A. E. Vazquez, E. N. Yamoah and N. Chiamvimonvat (2003). "Molecular identification and functional roles of a Ca(2+)-activated K+ channel in human and mouse hearts." J Biol Chem **278**(49): 49085-49094.

Yu, T., C. Deng, R. Wu, H. Guo, S. Zheng, X. Yu, Z. Shan, S. Kuang and Q. Lin (2012). "Decreased expression of small-conductance Ca2+-activated K+ channels SK1 and SK2 in human chronic atrial fibrillation." Life Sci **90**(5-6): 219-227.

Appendix A

Expression profile by qPCR of all genes investigated. All data are normalized. Abbreviations: RA: right atrium, LA: left atrium, RV: right ventricle, LV Endo: left ventricular endocardium, LV Mid: left ventricular midmyocardium, LV Epi: left ventricular epicardium.

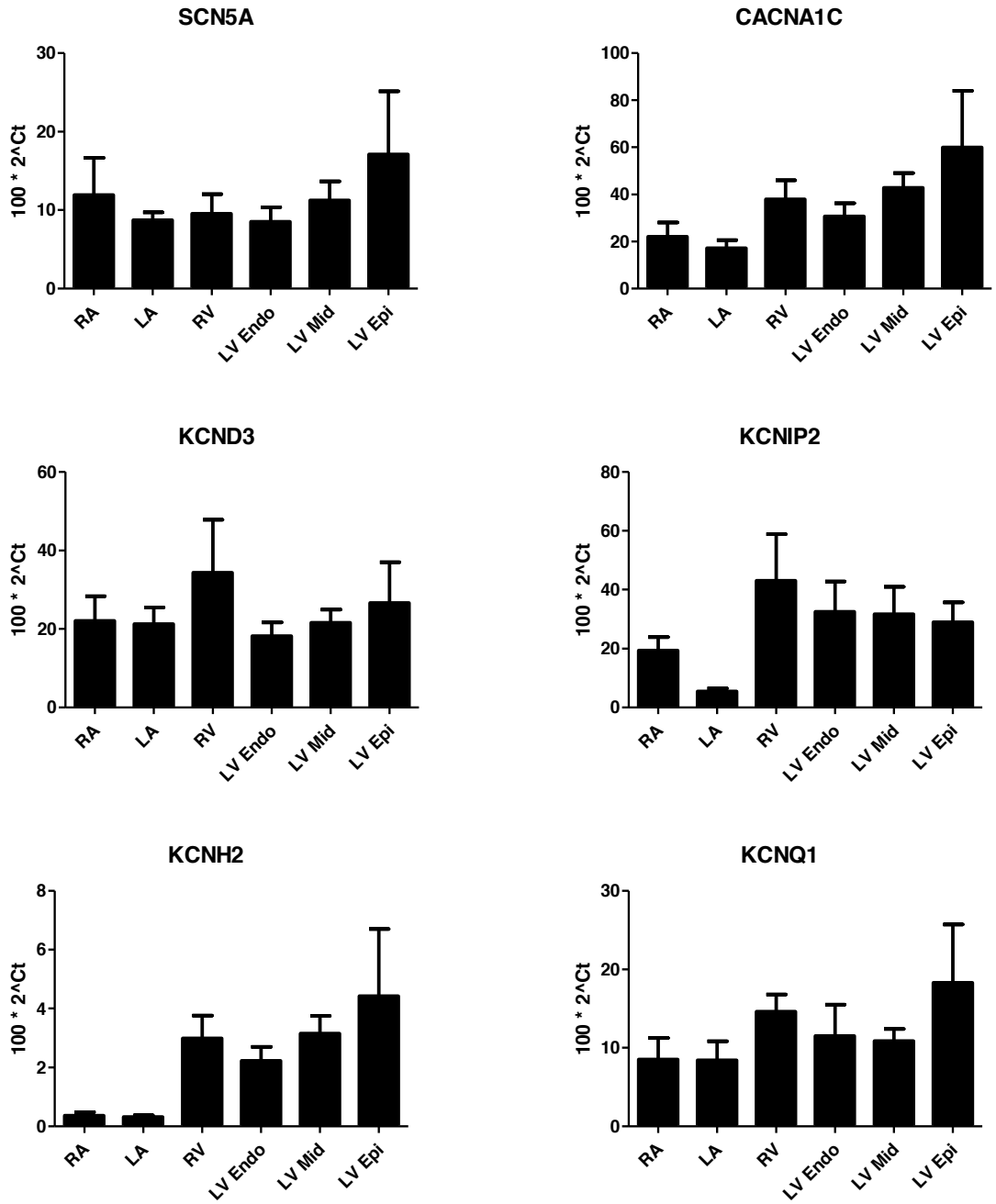

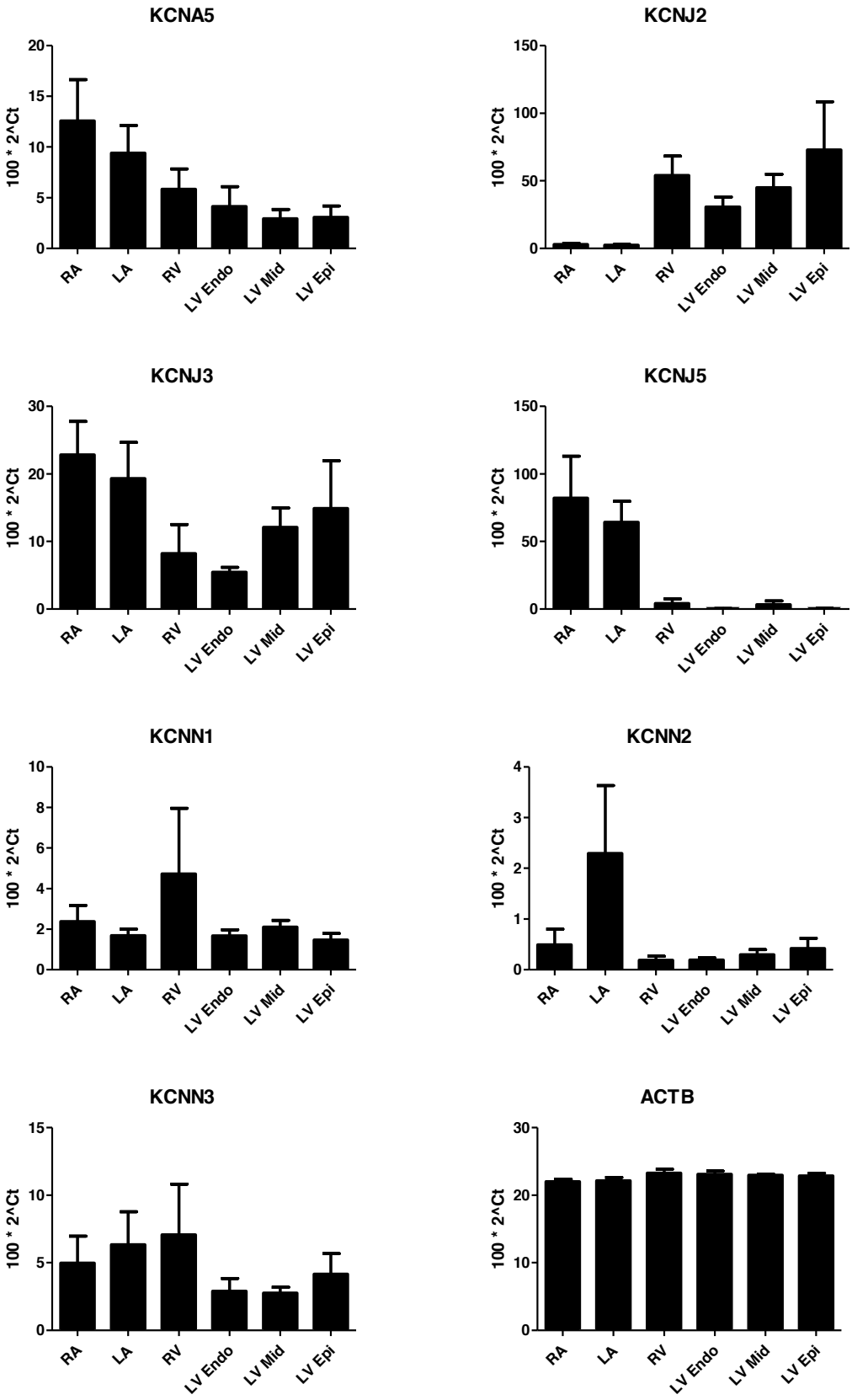
KCNA5
100 * 2^Ct
0
5
10
15
20
RA
LA
RV
LV Endo
LV Mid
LV Epi
KCNJ2
100 * 2^Ct
0
50
100
150
RA
LA
RV
LV Endo
LV Mid
LV Epi
KCNJ3
100 * 2^Ct
0
10
20
30
RA
LA
RV
LV Endo
LV Mid
LV Epi
KCNJ5
100 * 2^Ct
0
50
100
150
RA
LA
RV
LV Endo
LV Mid
LV Epi
KCNN1
100 * 2^Ct
0
2
4
6
8
10
RA
LA
RV
LV Endo
LV Mid
LV Epi
KCNN2
100 * 2^Ct
0
1
2
3
4
RA
LA
RV
LV Endo
LV Mid
LV Epi
KCNN3
100 * 2^Ct
0
5
10
15
RA
LA
RV
LV Endo
LV Mid
LV Epi
ACTB
100 * 2^Ct
0
10
20
30
RA
LA
RV
LV Endo
LV Mid
LV Epi

Original data of all genes investigated. $C_{t(gene)}$, $C_{t(ACTB)}$, ΔC_t and 2in delta ($100 * 2^{\Delta Ct}$) are presented. Number = horse, A= Right atrium, B= Left atrium, C= Right ventricle, D1= Left ventricular endocardium, D2= Left ventricular midmyocardium and D3= Left ventricular epicardium

	1A	1B	1C	1D1	1D2	1D3	2A	2B	2C	2D1	2D2	2D3	3A	3B	3C1	3D1	3D2	3D3	6A	6B	6C	6D1	6D2	6D3	10A	10B	10C	10D1	10D2	10D3	11A	11B	11C	11D1	11D2	11D3
SCN5A	25,11	25,7	25,72	26,01	25,82	26,63	27,19	25,99	28,73	27,08	27,44	26,45	25,11	27,38	28,84	28,86	25,82	25,34	26,24	25,18	26,52	25,54	27,23	26,36	25,61	25,26	26,17	27,13	26,6	25,78	24,42	24,78	25,33	26,51	25,03	25,28
ACTB	21,9	22,55	21,75	22,99	23,09	23,08	21,78	22,16	23,81	22,9	23,24	22,45	23,54	23,94	25,93	25,28	23,22	24,51	21,53	21,63	22,93	22,78	22,58	21,91	21,76	22,12	22,08	21,88	23,06	22,72	21,58	20,42	23,02	22,79	22,55	22,54
Delta	3,217	3,151	3,97	3,017	2,738	3,553	5,41	3,834	4,922	4,185	4,197	3,998	1,564	3,444	2,918	3,58	2,608	0,825	4,715	3,551	3,59	2,756	4,649	4,454	3,85	3,139	4,092	5,249	3,541	3,067	2,84	4,359	2,315	3,716	2,478	2,745
2in delta	10,76	11,26	6,383	12,35	14,99	8,522	2,353	7,01	3,298	5,499	5,452	6,261	33,81	9,192	13,23	8,363	16,4	56,46	3,808	8,529	8,302	14,8	3,985	4,564	6,935	11,35	5,864	2,63	8,591	11,93	13,97	4,872	20,09	7,608	17,95	14,92

	1A	1B	1C	1D1	1D2	1D3	2A	2B	2C	2D1	2D2	2D3	3A	3B	3C1	3D1	3D2	3D3	6A	6B	6C	6D1	6D2	6D3	10A	10B	10C	10D1	10D2	10D3	11A	11B	11C	11D1	11D2	11D3
KCNQ1	25,73	25,12	25,1	27,35	26,02	25,67	25,93	26,2	26,73	26,45	26,5	25,91	25,74	26,7	28,19	27,02	25,99	25,38	26,46	26,33	25,21	26,9	27,21	26,11	25,62	26,18	25,71	26,21	26	25,63	25,51	25,5	25,75	25,54	25,85	25,76
ACTB	21,9	22,55	21,75	22,99	23,09	23,08	21,78	22,16	23,81	22,9	23,24	22,45	23,54	23,94	25,93	25,28	23,22	24,51	21,53	21,63	22,93	22,78	22,58	21,91	21,76	22,12	22,08	21,88	23,06	22,72	21,58	20,42	23,02	22,79	22,55	22,54
Delta	3,839	2,562	3,353	4,359	2,938	2,587	4,149	4,038	2,914	3,552	3,254	3,459	2,199	2,761	2,262	1,735	2,778	0,874	4,93	4,699	2,278	4,119	4,628	4,199	3,854	4,067	3,633	4,329	2,94	2,91	3,931	5,086	2,73	2,752	3,301	3,221
2in delta	6,988	16,94	9,785	4,873	13,05	16,64	5,635	6,087	13,27	8,524	10,48	9,096	21,77	14,75	20,85	30,05	14,58	54,55	3,281	3,85	20,62	5,754	4,044	5,446	6,914	5,965	8,061	4,977	13,03	13,3	6,558	2,945	15,07	14,85	10,15	10,73

	1A	1B	1C	1D1	1D2	1D3	2A	2B	2C	2D1	2D2	2D3	3A	3B	3C1	3D1	3D2	3D3	6A	6B	6C	6D1	6D2	6D3	10A	10B	10C	10D1	10D2	10D3	11A	11B	11C	11D1	11D2	11D3
KCNA5	25,72	24,71	28,19	29,47	28,06	28,77	26,25	26,99	30,37	29,07	29,82	30,4	25,27	27,72	28,94	29,95	28,82	28,96	25,41	25,72	27	28,03	28,29	28,08	25,41	25,78	26,94	27,46	28,56	28,14	23,98	23,81	26,19	25,66	26,34	26,21
ACTB	21,9	22,55	21,75	22,99	23,09	23,08	21,78	22,16	23,81	22,9	23,24	22,45	23,54	23,94	25,93	25,28	23,22	24,51	21,53	21,63	22,93	22,78	22,58	21,91	21,76	22,12	22,08	21,88	23,06	22,72	21,58	20,42	23,02	22,79	22,55	22,54
Delta	3,829	2,16	6,447	6,482	4,974	5,689	4,469	4,832	6,56	6,177	6,573	7,949	1,728	3,78	3,018	4,671	5,605	4,453	3,881	4,094	4,063	5,25	5,705	6,175	3,649	3,659	4,864	5,574	5,5	5,425	2,398	3,393	3,174	2,867	3,789	3,67
2in delta	7,038	22,37	1,146	1,119	3,182	1,938	4,515	3,51	1,06	1,383	1,05	0,405	30,18	7,28	12,35	3,926	2,055	4,566	6,785	5,857	5,983	2,628	1,917	1,384	7,97	7,915	3,435	2,1	2,209	2,328	18,97	9,52	11,08	13,71	7,236	7,855

	1A	1B	1C	1D1	1D2	1D3	2A	2B	2C	2D1	2D2	2D3	3A	3B	3C1	3D1	3D2	3D3	6A	6B	6C	6D1	6D2	6D3	10A	10B	10C	10D1	10D2	10D3	11A	11B	11C	11D1	11D2	11D3
KCNJ3	23,64	23,77	25,92	27,3	25,7	27,09	25,44	25,38	29,72	27,22	27,17	27,93	25,21	27,13	31,58	29,01	26,94	25,56	25,32	24,4	26,85	26,65	26,82	26,34	23,73	24,03	26,72	27,13	25,94	26,1	23,1	23,72	24,78	26,92	24,65	24,98
ACTB	21,9	22,55	21,75	22,99	23,09	23,08	21,78	22,16	23,81	22,9	23,24	22,45	23,54	23,94	25,93	25,28	23,22	24,51	21,53	21,63	22,93	22,78	22,58	21,91	21,76	22,12	22,08	21,88	23,06	22,72	21,58	20,42	23,02	22,79	22,55	22,54
Delta	1,746	1,222	4,172	4,316	2,615	4,012	3,664	3,219	5,907	4,326	3,93	5,481	1,667	3,195	5,656	3,722	3,727	1,05	3,794	2,769	3,918	3,867	4,235	4,429	1,962	1,916	4,645	5,241	2,877	3,384	1,525	3,302	1,765	4,132	2,099	2,447
2in delta	29,82	42,88	5,549	5,02	16,33	6,197	7,888	10,74	1,666	4,987	6,563	2,239	31,49	10,92	1,983	7,577	7,55	48,3	7,21	14,67	6,614	6,852	5,31	4,642	25,66	26,5	3,998	2,644	13,61	9,577	34,74	10,14	29,43	5,704	23,34	18,34

	1A	1B	1C	1D1	1D2	1D3	2A	2B	2C	2D1	2D2	2D3	3A	3B	3C1	3D1	3D2	3D3	6A	6B	6C	6D1	6D2	6D3	10A	10B	10C	10D1	10D2	10D3	11A	11B	11C	11D1	11D2	11D3
KCNJ5	22,62	22,88	31,79	34,36	25,65	31,93	23,62	23,37	31,7	32,92	34,29	32,27	22,32	24,75	28,13	34,76	31,11	33,25	22,57	22,8	31,02	30,14	36,82	31,77	22,97	21,69	32,22	29,99	29,59	29,72	21,91	22,27	28,79	30,5	28,58	29,38
ACTB	21,9	22,55	21,75	22,99	23,09	23,08	21,78	22,16	23,81	22,9	23,24	22,45	23,54	23,94	25,93	25,28	23,22	24,51	21,53	21,63	22,93	22,78	22,58	21,91	21,76	22,12	22,08	21,88	23,06	22,72	21,58	20,42	23,02	22,79	22,55	22,54
Delta	0,721	0,332	10,04	11,37	2,567	8,851	1,839	1,216	7,892	10,03	11,05	9,826	-1,22	0,815	2,207	9,472	7,893	8,737	1,045	1,173	8,082	7,361	14,24	9,862	1,207	-0,42	10,14	8,105	6,525	7,009	0,333	1,849	5,774	7,708	6,03	6,846
2in delta	60,68	79,47	0,095	0,038	16,87	0,217	27,95	43,04	0,421	0,096	0,047	0,11	232,8	56,83	21,66	0,141	0,421	0,234	48,46	44,36	0,369	0,608	0,005	0,107	43,32	134	0,089	0,363	1,086	0,777	79,38	27,76	1,828	0,478	1,53	0,87

	1A	1B	1C	1D1	1D2	1D3	2A	2B	2C	2D1	2D2	2D3	3A	3B	3C1	3D1	3D2	3D3	6A	6B	6C	6D1	6D2	6D3	10A	10B	10C	10D1	10D2	10D3	11A	11B	11C	11D1	11D2	11D3
KCNJ2	28,01	27,53	23,43	25,08	24,73	24,24	27,87	28,8	26,44	25,17	24,73	24,44	27,6	29,17	25,8	26,2	23,58	23,21	27,56	28,24	24,35	25,83	25,65	25,09	27,59	26,56	23,15	24,13	24,14	23,14	25,75	25,96	23,29	23,68	23,15	23,98
ACTB	21,9	22,55	21,75	22,99	23,09	23,08	21,78	22,16	23,81	22,9	23,24	22,45	23,54	23,94	25,93	25,28	23,22	24,51	21,53	21,63	22,93	22,78	22,58	21,91	21,76	22,12	22,08	21,88	23,06	22,72	21,58	20,42	23,02	22,79	22,55	22,54
Delta	6,116	4,977	1,682	2,092	1,64	1,161	6,092	6,64	2,63	2,274	1,491	1,993	4,062	5,233	-0,12	0,917	0,368	-1,3	6,035	6,611	1,415	3,05	3,07	3,178	5,829	4,441	1,073	2,242	1,073	0,422	4,168	5,537	0,269	0,887	0,6	1,448
2in delta	1,442	3,176	31,16	23,46	32,09	44,71	1,466	1,002	16,15	20,67	35,59	25,13	5,986	2,66	108,8	52,97	77,47	245,6	1,525	1,023	37,49	12,08	11,91	11,05	1,76	4,605	47,54	21,14	47,53	74,64	5,563	2,154	83	54,06	66	36,66

	1A	1B	1C	1D1	1D2	1D3	2A	2B	2C	2D1	2D2	2D3	3A	3B	3C	3D1	3D2	3D3	6A	6B	6C	6D1	6D2	6D3	10A	10B	10C	10D1	10D2	10D3	11A	11B	11C	11D1	11D2	11D3
KCNIP2	23,92	26,67	23,61	24,97	24,26	23,87	24,88	26,53	26,03	23,9	24,82	24,88	24,93	29,48	28,24	27,99	25,98	26,37	23,93	26,09	23,32	24,7	24,91	24,48	24,42	25,9	25,84	26,46	26,73	25,36	25,44	23,96	22,94	23,23	23,08	23,96
ACTB	21,9	22,55	21,75	22,99	23,09	23,08	21,78	22,16	23,81	22,9	23,24	22,45	23,54	23,94	25,93	25,28	23,22	24,51	21,53	21,63	22,93	22,78	22,58	21,91	21,76	22,12	22,08	21,88	23,06	22,72	21,58	20,42	23,02	22,79	22,55	22,54
Delta	2,027	4,117	1,859	1,984	1,169	0,788	3,1	4,375	2,216	1,005	1,575	2,428	1,388	5,544	2,316	2,707	2,759	1,856	2,397	4,462	0,386	1,919	2,328	2,571	2,651	3,787	3,765	4,573	3,664	2,648	3,863	3,539	-0,08	0,436	0,526	1,425
2in delta	24,54	5,762	27,56	25,28	44,47	57,91	11,66	4,82	21,52	49,84	33,57	18,58	38,21	2,143	20,09	15,31	14,77	27,63	18,99	4,537	76,51	26,44	19,92	16,83	15,92	7,245	7,356	4,201	7,891	15,95	6,871	8,601	105,5	73,91	69,47	37,24

	1A	1B	1C	1D1	1D2	1D3	2A	2B	2C	2D1	2D2	2D3	3A	3B	3C	3D1	3D2	3D3	6A	6B	6C	6D1	6D2	6D3	10A	10B	10C	10D1	10D2	10D3	11A	11B	11C	11D1	11D2	11D3
KCND3	24,79	24,57	24,61	26,01	24,99	25,28	24,91	24,02	26,23	25,32	25,93	25,85	24,48	25,4	25,93	27,01	25,04	24,9	24,55	24,95	25,35	26,11	26,11	25,66	23,91	24,43	24,38	25,01	25,23	24,61	23,87	23,84	24,54	24,69	24,37	25
ACTB	21,9	22,55	21,75	22,99	23,09	23,08	21,78	22,16	23,81	22,9	23,24	22,45	23,54	23,94	25,93	25,28	23,22	24,51	21,53	21,63	22,93	22,78	22,58	21,91	21,76	22,12	22,08	21,88	23,06	22,72	21,58	20,42	23,02	22,79	22,55	22,54
Delta	2,889	2,02	2,868	3,025	1,904	2,205	3,132	1,866	2,419	2,427	2,69	3,4	0,938	1,466	-0	1,729	1,825	0,394	3,022	3,321	2,414	3,334	3,524	3,75	2,15	2,312	2,302	3,127	2,164	1,896	2,297	3,426	1,527	1,903	1,815	2,461
2in delta	13,5	24,66	13,7	12,29	26,72	21,69	11,4	27,44	18,71	18,6	15,5	9,471	52,2	36,19	100	30,17	28,23	76,11	12,31	10,01	18,76	9,917	8,693	7,431	22,53	20,14	20,28	11,44	22,32	26,87	20,35	9,304	34,69	26,74	28,42	18,16

	1A	1B	1C	1D1	1D2	1D3	2A	2B	2C	2D1	2D2	2D3	3A	3B	3C	3D1	3D2	3D3	6A	6B	6C	6D1	6D2	6D3	10A	10B	10C	10D1	10D2	10D3	11A	11B	11C	11D1	11D2	11D3
CACNA1C	24,47	24,3	23,89	25,19	24,3	24,06	25,32	25,16	25,32	24,77	24,56	24,23	24,58	25,95	26,33	26,11	23,97	23,68	24,8	24,78	24,44	24,76	25,25	24,5	24,14	24,71	24,2	24,23	23,93	23,71	23,39	23,99	24,46	24,35	23,74	24,02
ACTB	21,9	22,55	21,75	22,99	23,09	23,08	21,78	22,16	23,81	22,9	23,24	22,45	23,54	23,94	25,93	25,28	23,22	24,51	21,53	21,63	22,93	22,78	22,58	21,91	21,76	22,12	22,08	21,88	23,06	22,72	21,58	20,42	23,02	22,79	22,55	22,54
Delta	2,576	1,745	2,145	2,199	1,213	0,978	3,544	3	1,509	1,873	1,316	1,782	1,038	2,009	0,406	0,828	0,754	-0,83	3,27	3,154	1,51	1,976	2,672	2,591	2,379	2,598	2,124	2,347	0,869	0,991	1,817	3,576	1,444	1,563	1,189	1,485
2in delta	16,77	29,83	22,61	21,78	43,13	50,76	8,572	12,5	35,13	27,3	40,15	29,07	48,7	24,84	75,47	56,32	59,31	177,4	10,37	11,24	35,1	25,43	15,69	16,6	19,23	16,52	22,94	19,66	54,75	50,3	28,39	8,385	36,74	33,84	43,86	35,73

	1A	1B	1C	1D1	1D2	1D3	2A	2B	2C	2D1	2D2	2D3	3A	3B	3C	3D1	3D2	3D3	6A	6B	6C	6D1	6D2	6D3	10A	10B	10C	10D1	10D2	10D3	11A	11B	11C	11D1	11D2	11D3
KCNH2_2	30,37	30,85	28,7	28,81	28,16	28,93	30,93	30,76	27,96	28,48	28,58	28,73	30,51	31,5	30,41	29,78	27,44	27,19	31,32	29,51	28,19	28,62	29,12	28,35	30,92	30,76	28,63	28,43	27,63	27,39	28,82	29,74	27,92	28,24	27,73	27,68
ACTB	21,9	22,55	21,75	22,99	23,09	23,08	21,78	22,16	23,81	22,9	23,24	22,45	23,54	23,94	25,93	25,28	23,22	24,51	21,53	21,63	22,93	22,78	22,58	21,91	21,76	22,12	22,08	21,88	23,06	22,72	21,58	20,42	23,02	22,79	22,55	22,54
Delta	8,479	8,299	6,952	5,821	5,075	5,849	9,154	8,602	4,148	5,578	5,333	6,278	6,97	7,565	4,482	4,498	4,219	2,679	9,79	7,881	5,252	5,838	6,534	6,437	9,158	8,64	6,547	6,541	4,563	4,675	7,246	9,325	4,908	5,451	5,179	5,144
2in delta	0,28	0,317	0,808	1,769	2,967	1,735	0,176	0,257	5,641	2,093	2,481	1,288	0,798	0,528	4,476	4,426	5,369	15,61	0,113	0,424	2,624	1,748	1,079	1,155	0,175	0,251	1,069	1,074	4,231	3,916	0,659	0,156	3,331	2,286	2,761	2,827

	1A	1B	1C	1D1	1D2	1D3	2A	2B	2C	2D1	2D2	2D3	3A	3B	3C	3D1	3D2	3D3	6A	6B	6C	6D1	6D2	6D3	10A	10B	10C	10D1	10D2	10D3	11A	11B	11C	11D1	11D2	11D3
KCNN1	28,21	27,8	28,61	29,56	28,85	29,38	27,05	28,19	29,76	29,56	28,7	28,95	27,56	29,55	28,19	30,65	28,54	29,86	28,43	29,15	29,23	27,98	29,91	31,19	27,77	27,55	28,62	28,21	28,43	28,41	27,31	27,03	28,26	28,77	27,63	28,29
ACTB	21,9	22,55	21,75	22,99	23,09	23,08	21,78	22,16	23,81	22,9	23,24	22,45	23,54	23,94	25,93	25,28	23,22	24,51	21,53	21,63	22,93	22,78	22,58	21,91	21,76	22,12	22,08	21,88	23,06	22,72	21,58	20,42	23,02	22,79	22,55	22,54
Delta	6,31	5,249	6,859	6,574	5,764	6,3	5,267	6,033	5,949	6,661	5,46	6,502	4,022	5,612	2,261	5,366	5,325	5,345	6,904	7,524	6,292	5,197	7,324	9,279	6,003	5,431	6,539	6,323	5,364	5,69	5,73	6,608	5,24	5,978	5,081	5,758
2in delta	1,26	2,63	0,861	1,05	1,84	1,269	2,597	1,527	1,618	0,989	2,272	1,104	6,154	2,045	20,87	2,425	2,495	2,46	0,835	0,543	1,276	2,726	0,624	0,161	1,559	2,319	1,075	1,249	2,428	1,937	1,884	1,025	2,645	1,586	2,955	1,848

	1A	1B	1C	1D1	1D2	1D3	2A	2B	2C	2D1	2D2	2D3	3A	3B	3C	3D1	3D2	3D3	6A	6B	6C	6D1	6D2	6D3	10A	10B	10C	10D1	10D2	10D3	11A	11B	11C	11D1	11D2	11D3
KCNN2	32,58	26,11	32,1	32,52	31,82	31,86	33,36	31,19	33,84	32,57	32,49	31,78	30,49	28,78	33,38	33,2	31,3	30,66	33,14	29,65	33,1	32,43	33,91	32,62	31,69	29,05	31,24	31,29	31,26	30,5	27,48	30,14	31,8	30,86	30,16	30,69
ACTB	21,9	22,55	21,75	22,99	23,09	23,08	21,78	22,16	23,81	22,9	23,24	22,45	23,54	23,94	25,93	25,28	23,22	24,51	21,53	21,63	22,93	22,78	22,58	21,91	21,76	22,12	22,08	21,88	23,06	22,72	21,58	20,42	23,02	22,79	22,55	22,54
Delta	10,69	3,558	10,35	9,527	8,735	8,785	11,58	9,033	10,03	9,673	9,251	9,33	6,951	4,839	7,457	7,92	8,08	6,155	11,62	8,022	10,16	9,646	11,33	10,71	9,922	6,93	9,162	9,404	8,68	8,59	5,715	8,022	9,719	8,973	7,1	7,975
2in delta	0,061	8,49	0,076	0,136	0,235	0,227	0,033	0,191	0,095	0,122	0,164	0,155	0,808	3,494	0,569	0,413	0,369	1,404	0,032	0,385	0,087	0,125	0,039	0,06	0,103	0,82	0,175	0,148	0,244	0,259	1,904	0,385	0,119	0,199	0,729	0,398

KCNN3	1A	1B	1C	1D1	1D2	1D3	2A	2B	2C	2D1	2D2	2D3	3A	3B	3C	3D1	3D2	3D3	6A	6B	6C	6D1	6D2	6D3	10A	10B	10C	10D1	10D2	10D3	11A	11B	11C	11D1	11D2	11D3
	27,04	25,38	26,31	28,87	27,81	27,08	26,74	28,16	29,03	29,08	29,25	29,36	26,28	26,81	27,89	29,04	27,95	27,74	26,51	26,3	27,87	28,03	28,45	28,04	27,08	27,01	27,95	27,65	28,63	27,85	26,57	26,63	27,4	28,12	27,32	27,66
ACTB	21,9	22,55	21,75	22,99	23,09	23,08	21,78	22,16	23,81	22,9	23,24	22,45	23,54	23,94	25,93	25,28	23,22	24,51	21,53	21,63	22,93	22,78	22,58	21,91	21,76	22,12	22,08	21,88	23,06	22,72	21,58	20,42	23,02	22,79	22,55	22,54
Delta	5,141	2,824	4,561	5,88	4,728	4	4,963	6,001	5,218	6,18	6,007	6,911	2,74	2,87	1,961	3,755	4,737	3,226	4,983	4,669	4,94	5,254	5,865	6,132	5,313	4,894	5,87	5,765	5,567	5,133	4,996	6,211	4,38	5,325	4,772	5,119
2in delta	2,834	14,13	4,237	1,698	3,774	6,252	3,207	1,561	2,686	1,38	1,555	0,831	14,97	13,68	25,69	7,408	3,751	10,69	3,163	3,931	3,257	2,621	1,716	1,426	2,516	3,364	1,71	1,839	2,109	2,85	3,134	1,35	4,802	2,494	3,66	2,878

Appendix B

RNA purification using TriReagent

1. Add about 1ml of TriReagent to 100mg of tissue
2. Homogenize in 30 sec at 5500. Repeat 3 times. Keep samples on ice while the machine cools.
3. Transfer supernatant to 1,5ml eppendorftubes
4. Incubate 5 min at room temperature
5. Add 200ml chloroform (0,2ml per 1ml of TriReagent)
6. Shake vigorously for 15 seconds
7. Incubate 10 min in room temperature
8. Centrifugate at 12000x G for 15 min in 4°C
9. The aqueous phase (upper) is transferred to a new 1,5ml eppendorftube
10. Add 500 isopropanol (0,5ml per 1ml of TriReagent)
11. Mix by flipping the tube
12. Incubate 10 min in room temperature
13. Centrifugate at 12000xG for 10 min in 4°C
14. Remove the supernatant
15. Wash by adding 1ml 75% EtOH (1 ml per 1ml TriReagent)
16. Mix by flipping the tube
17. Centrifugate at 7,500xG for 5 min in 4°C
    (If pellet floats, centrifugate again at 12000xG for 5 min in 4°C)
18. Remove the supernatant
19. Wash by adding 1ml 75% EtOH (1ml per 1 ml TriReagent)
20. Mix by flipping the tube
21. Centrifugate at 7,500xG for 5min in 4°C
22. Remove the supernatant
23. Dry the RNA pellet for 10min (not completely dry!)
24. Add 50ul RNAse free H2O
25. Incubate for 15min at 55°C to completely dissolve the pellet
26. For longer storage, the samples should be at -80°C

Verification on 1% agarose gel

Mix 5µL RNA and 2µL RNA loading dye

Heat for 10 min at 65°C

Load on 1% agarose gel

Dilute samples to obtain a concentration of 0.2 µg/µL.

Reverse Transcriptase

RNA sample	40.0 µL
10 x RT buffer	8.0 µL
25 x dNTP mix	3.2 µL
10 x RT random primers	8.0 µL
Multiscribe Reverse Transcriptase	1.0 µL
RNase Inhibitor	2.0 µL
Nuclease Free H2O	17.8 µL
Total	80.0 µL

Leave the samples at room temperature for 10 min

Incubate the samples at 37°C for 120 min

Incubate the samples at 85°C for 10 sec

Add 500 µL H2O and aliquot the sample into 4 eppendorftubes ≈ 100 µL/tube

Real-time PCR

TaqMan Assay		1.0 µL
Sample	cDNA	9.0 µL
Gene Expression Master Mix		10.0 µL
Total		20.0 µL

Immunohistochemistry

Equine heart tissue

1. Leave the slices in PBS at room temperature for 10 min to rehydrate the dried tissue
2. Fixation: Immerse the slices in fresh (PFA-4% in PBS) for 20 min
3. Wash 2 times in PBS
4. Block 30 minutes at room temperature in PBS containing 0.2% triton X-100 + 4%BSA (PBS_bT)
5. Add primary antibody diluted PBS_bT. Incubate overnight at 4°C
6. Wash 3 times in PBS
7. Incubate with fluorochrome-coupled secondary antibody diluted in PBS_bT for 1 hour at room temperature
8. Wash 3 times in PBS
9. Mount sections in Prolong Gold

Primary antibodies employed:

Anti-Connexin 43, mouse monoclonal IgG_1 (Invitrogen, 35-5000) 1:200

Experiment 1: Anti-$K_{Ca}2.2$ (SK2), rabbit polyclonal (Alomone, APC-028) 1:200

Experiment 2: Anti-$K_{Ca}2.3$ (SK3), rabbit polyclonal (Alomone, APC-025) 1:200

Experiment 3: Anti-KCNN2, rabbit polyclonal (Sigma-Aldrich, SAB2101228) 1:200

Secondary antibodies employed:

AlexaFluor® 568 Goat Anti-Rabbit IgG (*Life Technologies*™ A-11011) 1:200

AlexaFluor® 488 Goat Anti-Mouse IgG_1 (*Life Technologies*™ A-21121) 1:200

DAPI nucleic acid stain (Invitrogen D-1306) 1:300

Abstract accepted for chaired poster presentation at ECAS congress, Munich 2014

In Vitro Characterization of the Equine Cardiac Ion Channels

Eva Zander Hesselkilde[1], Maria Mathilde Haugaard[1], Lasse Skibsbye[2], Rikke Buhl[1], Thomas Jespersen[2]

[1]Department of Large Animal Sciences, Faculty of Medicine and Health Sciences, University of Copenhagen, Denmark [2]Department of Biomedical Sciences, Faculty of Medicine and Health Sciences, University of Copenhagen

Increased focus on prevalence and causes of cardiac arrhythmias in horses has aroused in recent years. Unlike other animals, atrial fibrillation (AF) is a frequent arrhythmia in horse. Also, horses with non-diseased hearts can be electrical triggered into shorter and longer periods of AF. We have previously found that treatment with both blockers of the cardiac sodium channel and of small-conductance Ca^{2+}-activated K^+ (SK) channels can abrogate induced AF. Such pharmacological observations combined with a cardiac electrophysiology largely resembling the human suggest that equine hearts may constitute a *bona fida* model of human AF. To further investigate whether horses can be used to improve treatment of human arrhythmias knowledge about the equine cardiac ion channels are needed.

The aim of this study is to quantify the presence, expression level and cellular and regional distribution of the most prominent potassium and sodium ion channels in the horse heart. The genes of interest are: KCNN1 (SK1), KCNN2 (SK2), KCNN3 (SK3), KCND3 (Kv4.3), KCNJ2 (Kir2.1), KCNIP2 (KChiP2), KCNQ1 (Kv7.1), KCNA5 (Kv1.5), KCNJ3 (GIRK1), KCNJ5 (GIRK4), KCNH2 (ERG1), CACNA1C (Cav1.2), and SCN5A (Nav1.5).

Methods: Quantitative real time PCR (qPCR) was conducted on cardiac tissue collected from 6 different atrial (RA and LA) and ventricular (RV and endo, mid and epi LV) locations from 6 euthanized horses (3.4 ± 0.2 kg) Immunohistochemistry was performed on 12 µm cryosections from both left and right atrial and ventricular preparation. SK2 channels were stained with a previously tested SK2-antibody, to document distribution and localization of this protein in the equine heart.

Results: Quantifications of the major cardiac ion channels in the equine heart revealed an expression pattern which to a large extent resembles the human expression profile. These results thereby support the resemblance between human and equine hearts.

In Vitro Characterization of the Equine Cardiac Ion Channels

Eva Zander Hesselkilde[1], Maria Mathilde Haugaard[1], Lasse Skibsbye[2], Rikke Buhl[1], Thomas Jespersen[2]

[1]Department of Large Animal Sciences, Faculty of Medicine and Health Sciences, University of Copenhagen, Denmark [2]Department of Biomedical Sciences, Faculty of Medicine and Health Sciences, University of Copenhagen

Abstract

Introduction: Increased focus on prevalence and causes of cardiac arrhythmias in horses has aroused in recent years. Unlike other animals, atrial fibrillation (AF) is a frequent arrhythmia in horses. Also, horses with non-diseased hearts can be electrically triggered into shorter and longer periods of AF. We have previously found that treatment with both blockers of the cardiac sodium channel and of small-conductance Ca^{2+}-activated K^+ (SK) channels can abrogate induced AF. Such pharmacological observations combined with a cardiac electrophysiology largely resembling the human suggest that equine hearts may constitute a *bona fida* model of human AF. To further investigate whether horses can be used to improve treatment of human arrhythmias knowledge about the equine cardiac ion channels are needed.

The aim of this study is to quantify the presence, expression level and cellular and regional distribution of the most prominent potassium and sodium ion channels in the equine heart. The aim of this study is to quantify the presence, expression level and cellular and regional distribution of the most prominent potassium and sodium ion channels in the horse heart. The genes of interest are: KCNN1 (SK1), KCNN2 (SK2), KCNN3 (SK3), KCND3 (Kv4.3), KCNJ2 (Kir2.1), KCNIP2 (KChiP2), KCNQ1 (Kv7.1), KCNA5 (Kv1.5), KCNJ3 (GIRK1), KCNJ5 (GIRK4), KCNH2 (ERG1), CACNA1C (Cav1.2), and SCN5A (Nav1.5).

Methods: Quantitative real time PCR (qPCR) was conducted on cardiac tissue collected from 6 different atrial (RA and LA) and ventricular (RV and LV Endo, LV Mid and LV Epi) locations from 6 euthanized horses (3.4 ± 0.2 kg) Immunohistochemistry was performed on 12 µm cryosections from both left and right atrial and ventricular preparation. SK2 channels were stained with a previously tested SK2-antibody, to document distribution and localization of this protein in the equine heart.

Results: Quantifications of the major cardiac ion channels in the equine heart revealed an expression pattern which to a large extent resembles the human expression profile. These results thereby support the resemblance between human and equine hearts.

	RA		LA		RV		LV Endo		LV Mid		LV Epi	
	Average	SEM	Average	SEM	Average	SEM	Average	SEM	Average	SEM	Average	SEM
SCN5A	11.94	4.7	8.70	1.1	9.53	2.5	8.54	1.8	11.23	2.4	17.11	8.0
KCNH2	0.37	0.1	0.32	0.1	2.99	0.8	2.23	0.5	3.15	0.6	4.42	2.3
KCNQ1	8.53	2.7	8.42	2.4	14.61	2.2	11.50	4.0	10.89	1.5	18.29	7.4
KCNA5	12.58	4.1	9.41	2.7	5.84	2.0	4.14	2.0	2.94	0.9	3.08	1.1
KCNJ3	22.80	5.0	19.31	5.3	8.21	4.3	5.46	0.7	12.12	2.9	14.88	7.1
KCNJ5	82.10	31.0	64.24	15.63	4.08	3.5	0.29	0.1	3.33	2.7	0.39	0.1
KCNN1	2.38	0.8	1.68	0.3	4.72	3.2	1.67	0.3	2.10	0.3	1.46	0.3
KCNN2	0.49	0.3	2.29	1.3	0.19	0.1	0.19	0.04	0.30	0.1	0.42	0.2
KCNN3	4.97	2.0	6.34	2.4	7.06	3.8	2.91	0.9	2.76	0.4	4.15	1.5
KCNJ2	2.96	0.9	2.44	0.6	54.02	14.3	30.73	7.4	45.10	9.8	72.96	35.6
KCNIP2	19.37	4.5	5.52	0.9	43.09	15.8	32.50	10.3	31.68	9.3	29.02	6.7
KCND3	22.05	6.3	21.29	4.3	34.36	13.4	18.19	3.5	21.65	3.3	26.62	10.3
CACNA1C	22.00	6.1	17.22	3.4	38.00	7.9	30.72	5.5	42.82	6.2	59.98	24.1
ACTB	22.01	0.3	22.14	0.5	23.25	0.6	23.10	0.5	22.96	0.1	22.87	0.4

Table 1. Normalized data from real-time PCR with beta-actin (ACTB) as reference gene. Units for all expression values are $100 * 2^{-\Delta Ct}$. n= 6. Abbreviations: RA: right atrium, LA: left atrium, RV: right ventricle, LV Endo: left ventricular endocardium, LV Mid: left ventricular midmyocardium, LV Epi: left ventricular epicardium.

Fig. 1. Horse in dorsal recumbency during NS8593 experiment

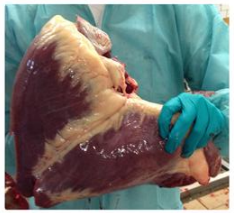

Fig. 2. Equine heart

In vivo effects of SK-block

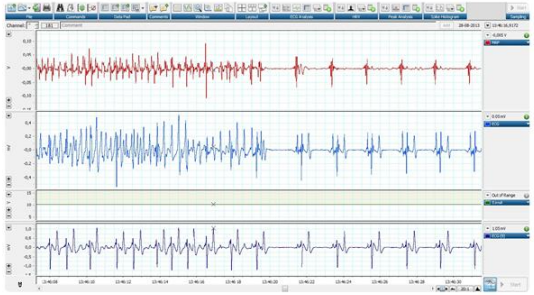

Fig. 3. ECG recordings of a horse converting from induced AF to sinus rhythm 10 minutes after treatment with NS8593 (5mg/kg). From top: Intra-atrial lead, P-wave lead and modified base-apex lead.

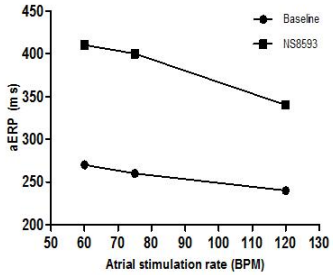

Fig. 4. Atrial effective refractory period (aERP) measured pre and post introduction to NS8593

qPCR

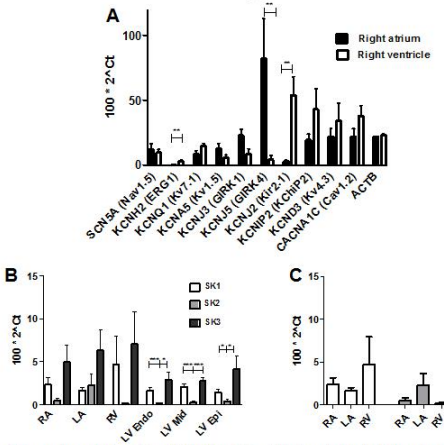

Fig. 5. Expression profile by real-time PCR of Na^+, Ca^{2+} and K^+ channel subunits in the equine heart. **A**: Comparision of right atrium and right ventricle. **B**: Relative distribution of the three isoforms of SK channels in the right atrium, left atrium, right ventricle and left ventricular endo-, mid and epicardium. **C**: Relative distribution of SK1, SK2 and SK3 with in RA, LA and RV.

Immunohistochemistry

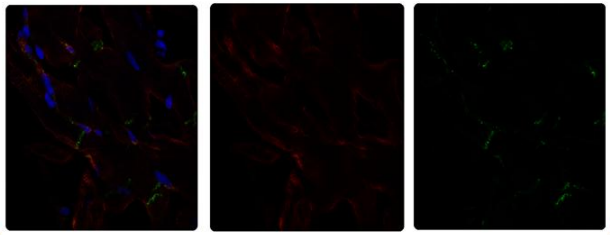

Fig. 6. Staining of right atrial cardiomyocytes using specific SK2 antibodies. Blue: DAPI, green: CX43, red: SK2

Conclusion

- The ion channel distribution of the horse largely resembles the human expression profile
- No significant difference of KCNA5 (Kv1.5) transcript between atria and ventricles
- Overall low expression level of KCNH2 (ERG1) but significant more in the ventricles

- All three isoform of SK channels are present in equine heart
- SK2 is expressed significant less than SK1 and SK3 except in the left atrium
- Positive staining results can be obtained using human SK2 antibodies